Validation of EarthCARE/ATLID aerosol profiling products with ground-based PollyNET lidars – case studies

Holger Baars[1], Moritz Haarig[1], Leonard König[1], Athena A. Floutsi[1], Elizaveta Basharova[1], Julian Hofer[1], Henriette Gebauer[1], Ronny Engelmann[1], Dietrich Althausen[1], Annett Skupin[1], Benedikt Gast[1], Felix Fritzsch[1], Kevin Ohneiser[1], Cristofer Jimenez[1], Tom Gaudek[1], Martin Radenz[1], Håvard Buholdt[1], Birgit Heese[1], Andi Klamt[1], Patric Seifert[1], David P. Donovan[2], Gerd-Jan van Zadelhoff[2], Sabur F. Abdullaev[3], Shohina K. Khalifaeva[3], Dilovar F. Nozirov[3], and Ulla Wandinger[1]

[1]Leibniz Institute for Tropospheric Research (TROPOS), Leipzig, Germany
[2]Royal Netherlands Meteorological Institute (KNMI), de Bilt, the Netherlands
[3]Physical Technical Institute of the Academy of Sciences of Tajikistan, Dushanbe, Tajikistan

Correspondence: Holger Baars (baars@tropos.de)

Abstract. The satellite mission EarthCARE (Earth Cloud, Aerosol, and Radiation Explorer) of the European Space Agency (ESA) and the Japan Aerospace Exploration Agency (JAXA) was successfully launched in May 2024. The satellite has four instruments on board, namely a high-spectral-resolution lidar called ATLID, a Cloud Profiling Doppler Radar (CPR), a Multi-Spectral Imager (MSI), and a Broad-Band Radiometer (BBR). ATLID provides for the first time directly measured profiles of the extinction and backscatter coefficient (and thus lidar ratio) together with the depolarization ratio at 355 nm from space. Since the start of the measurements, several updates in the ESA's processing chain have been made resulting in different baselines of the products. A first homogenized data set for the entire mission duration processed with one algorithm version, namely Baseline BA, was accomplished in September 2025. We used ground-based multiwavelength-Raman-polarization lidars of PollyNET operating in the framework of the Aerosol, Clouds and Trace gases Research Infrastructure (ACTRIS) to discuss the quality of ATLID profiling products based on golden case studies. The PollyNET lidars measure the same geophysical parameter as EarthCARE, namely profiles of the particle backscatter coefficient, the particle extinction coefficient, and the particle linear depolarization ratio at 355 nm. Seven dedicated cases, for which EarthCARE and the ground-based reference system observed the same atmospheric scene, were selected, spanning several atmospheric conditions (ice clouds, high aerosol load, pristine conditions) and geographic locations (Tropical Atlantic, Europe, Central Asia, and the pristine Southern Hemisphere). Our investigations revealed that ATLID has remarkable profiling capabilities with good signal strength and high vertical resolution. The ATLID profiling product of ESA's processing chain, A-EBD, could resolve the vertical structure of the targeted atmospheric features very well so that the A-EBD backscatter and extinction profiles (at low resolution) matched qualitatively (and mostly quantitatively) with the ground-based reference observations for most investigated atmospheric conditions. The intensive particle quantity lidar ratio is retrieved layer-wise and thus not in the same resolution as the backscatter and extinction products. It matches in many cases with the ground-based reference, but we also detected occasions when the lidar ratio in certain atmospheric regions was significantly deviating from the reference, which also then affects either the extinction or backscatter coefficient values. Especially edge effects at the transition of particle layers to clean air seem to be problematic.

Concerning ATLID's depolarization ratio, fair agreement was found for strongly scattering and depolarizing features, like ice clouds – especially during nighttime. For the aerosol regime, however, we confirm significant deviations from the ground reference and consider the depolarization ratio in Baselines BA and BB as quantitatively not reliable, especially during daytime. Thus, ATLID's depolarization ratio of Baselines B can be used to discriminate but not to type atmospheric features.

In conclusion, we can state that ATLID's optical profiles of Baselines B are ready for scientific exploitation keeping in mind the reported drawbacks (e.g., depolarization ratio offsets, edge effects, occasional retrieval errors, non-complete quality flags). EarthCARE data should therefore be intensively quality checked before using for scientific studies. As EarthCARE's lifetime was recently foreseen to last for more than 10 years and algorithm development continues, such validation efforts stay important and complement other respective validation approaches.

1 Introduction

The Earth Cloud, Aerosol, and Radiation Explorer (EarthCARE) is a satellite mission developed by the European Space Agency (ESA) in cooperation with the Japan Aerospace Exploration Agency (JAXA) which measures vertical profiles of aerosol, cloud, and precipitation properties together with the top of atmosphere (TOA) radiative fluxes (Wehr et al., 2023). This Earth Explorer mission was launched in May 2024 and observes the atmosphere using a high-spectral-resolution lidar (HSRL), a Doppler cloud radar, a multi-spectral imager and a broadband radiometer.

The active instruments (i.e., lidar and radar) provide detailed vertical information on aerosols and clouds with a narrow footprint (like atmospheric curtains), while the multi-spectral imager gives the horizontal context of the scene (like a carpet) by measuring spectral radiancies at the top of the atmosphere. Together, these synergistic observations aim to enhance our understanding of aerosols, clouds, and radiation and their interactions. Finally, radiative closure with the corresponding broadband radiometer measurements is envisaged, enabling near–real-time evaluation of the retrieved atmospheric state, with particular emphasis on cloud and aerosol properties and their radiative effects.

The atmospheric lidar (ATLID) on board EarthCARE is a polarization HSRL operating at a wavelength of 355 nm (do Carmo et al., 2021). It is the first time that the lidar (extinction-to-backscatter) ratio and the depolarization ratio at this wavelength can be measured simultaneously and directly from space, allowing for independent aerosol typing (Wandinger et al., 2023a). Being a novel instrument in space, extensive validation activities for the instrument (Level 1 data), as well as for the derived products (Level 2 data) are needed (e.g., Kubota et al., 2026; Wandinger et al., 2024).

Amiridis et al. (2025) recently prepared a Best Practice Protocol for the Validation of Aerosol, Cloud, and Precipitation Profiles measured from space in the framework of the Committee on Earth Observation Satellites (CEOS), taking into account lessons learned from previous spaceborne lidar activities such as the Cloud-Aerosol Lidar and Infrared Pathfinder Satellite Observations (CALIPSO) mission launched in 2006 (Winker et al., 2010), the Cloud-Aerosol Transport System (CATS) operating in 2015 (Yorks et al., 2016), the Aeolus Earth Explorer mission launched in 2018 (Stoffelen et al., 2005; Reitebuch, 2025), and the Aerosol and Carbon Detection Lidar (ACDL, Dai et al., 2024) on DQ-1 launched in 2022. The authors of the best practice document intensively discussed the different validation approaches for spaceborne lidars such as:

- dedicated airborne campaigns (e.g., Rogers et al., 2011; Witschas et al., 2020; Lux et al., 2020; Bedka et al., 2021; Flamant et al., 2024; Trapon et al., 2025; Groß et al., 2026),
- large field campaigns (e.g., Ansmann et al., 2011; Tesche et al., 2013; Weinzierl et al., 2017; Fehr et al., 2023; Marinou et al., 2023),
- satellite-to-satellite validation (e.g., Redemann et al., 2012; Kim et al., 2013; Feofilov et al., 2022),
- near-real-time (NRT) validation through monitoring in an assimilation system (e.g., Fielding and Janisková, 2020; Janisková and Fielding, 2020; Marseille et al., 2022; Bley et al., 2022),
- statistical comparisons with data from existing ground-based sites and networks (e.g., Pappalardo et al., 2010; Thorsen et al., 2011; Omar et al., 2013; Papagiannopoulos et al., 2016; Proestakis et al., 2019; Baars et al., 2023; Sun et al., 2023; Voudouri et al., 2024; Liu et al., 2024),
- but also case-study-based analysis (e.g., Mamouri et al., 2009; Wu et al., 2011; Kanitz et al., 2014; Pauly et al., 2019; Baars et al., 2020, 2021; Gkikas et al., 2023; Paschou et al., 2025)

and how they complement each other.

In this work, we focus on dedicated case studies using ground-based lidars to provide a first overview of the potentials and limitations of the ATLID profiling products. This case study approach allows us to discuss in detail the features and challenges of the mission with its complex processing chain with respect to aerosol profiling, and can thus be seen as a complement to the other validation approaches for EarthCARE. A similar approach was performed by Liu et al. (2024) for the validation of the novel Chinese spaceborne HSRL at 532 nm (ACDL, Dai et al., 2024) using six overpasses over ground-based lidar stations, which also demonstrated how valuable the intensive analysis of dedicated case studies for the validation of spaceborne lidar is.

The Leibniz Institute for Tropospheric Research (TROPOS) is strongly involved in the EarthCARE Calibration/Validation (Cal/Val) activities and operates (mobile) ground-based multiwavelength-Raman-polarization lidar systems (PollyXT, Engelmann et al., 2016, 2025) around the globe within the framework of PollyNET (Baars et al., 2016; Heese et al., 2025). All of these systems are part of ACTRIS/EARLINET (Laj et al., 2024; Pappalardo et al., 2014) and participated in the ATMO-ACCESS pilot project for the preparation of EarthCARE validation activities (Baars et al., 2024; Marinou et al., 2024). While the ACTRIS and ATMO-ACCESS ground-based stations cover more than 40 ground-based sites mainly distributed across Europe, here we concentrate on dedicated golden case studies with PollyNET lidar measurements taken at several locations around the globe (see Fig. 1) making also use of the ACTRIS mobile facilities OCEANET (shipborne, Bohlmann et al., 2018; Radenz et al., 2024) and LACROS (land-based, Radenz et al., 2021a). In this way, we provide a first glimpse on the observing capabilities of ATLID's geophysical products provided by ESA (see Sec. 2.1) and discuss their potentials as well as current limitations.

For the validation of ATLID profiling products, seven atmospheric scenes have been carefully selected to cover a wide range of atmospheric conditions and geographical regions. The observations span from dust and smoke events to ice clouds and very

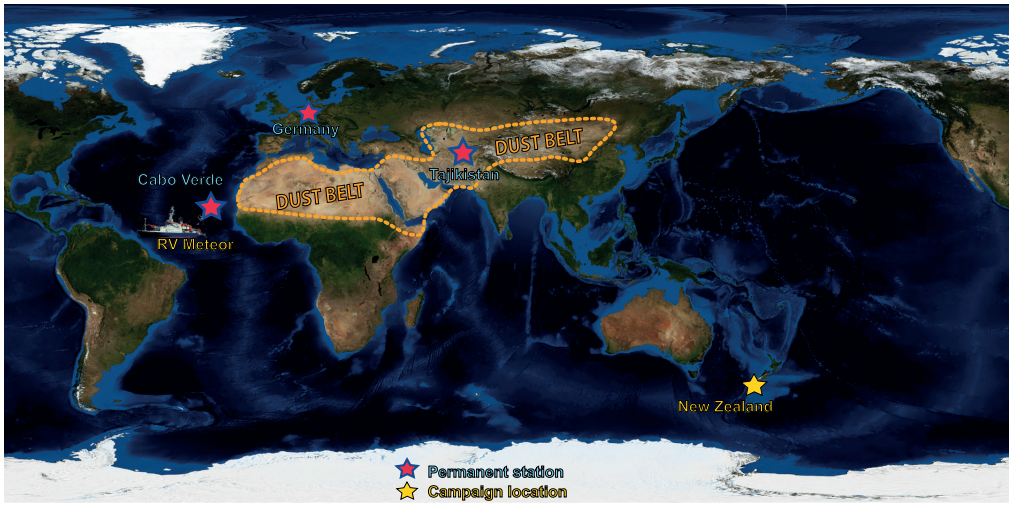

Figure 1. Map of locations of ground-based PollyNET lidar observations used for ATLID validation. Map source: NASA/Goddard Space Flight Center Scientific Visualization Studio. The Blue Marble Next Generation data is courtesy of Reto Stöckli (NASA/GSFC) and NASA's Earth Observatory.

pristine conditions, covering the Tropical Atlantic, Europe, Central Asia, and the pristine Southern Hemisphere. The selected case studies are characterized by EarthCARE overpasses in very close vicinity to the ground site (closest distance less than 20 km distance for all except of one) and atmospheric conditions representative for validation according to the discussion of scene homogeneity (Amiridis et al., 2025).

Both space agencies have set up their own processing chain (e.g., Eisinger et al., 2024; Nishizawa et al., 2026), providing independent products. In this work, we focus on the products from the processing chain of ESA. In this processing chain, EarthCARE data is structured into separate levels available for users: Level 1 data comprises calibrated instrument data, while Level 2 data comprises retrieved geophysical data products. The latter is divided into products using a single instrument only (L2A) and products utilizing synergistic measurements of 2 or more instruments (L2B). While ATLID Level 1 data (Eisinger et al., 2024) have been intensively validated in the early phase of the EarthCARE mission (Donovan, 2025; Haarig et al., 2025b; Groß et al., 2026), the focus of this work is on the ATLID L2A profiling products (Donovan et al., 2024). We analyzed Baseline BA, i.e., the algorithm version of the ESA EarthCARE processing chain that has been used to reprocess the entire data set of EarthCARE from August 2024 to September 2025, except for the last case for which the more recent Baseline BB was already applied. Where possible, we compared the results with earlier baselines to explain and discuss changes in the retrieval chain, which have been already implemented to improve the products.

The paper is structured as follows: First, ATLID, the ground-based instruments, and their data products are introduced together with a description of the measurement sites (Sec. 2). Then, seven validation cases are intensively discussed (Sec. 3), before drawing conclusions on ATLID products of Baseline BA to BB in Sec. 4.

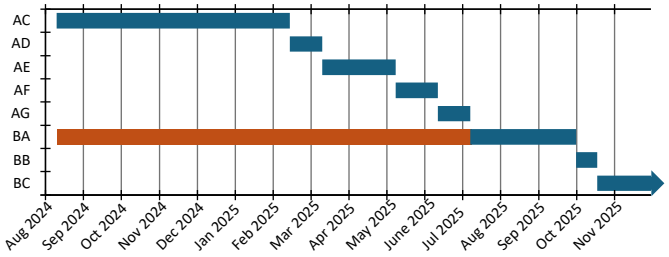

Figure 2. Overview of the algorithm versions (baselines) deployed for A-PRO from August 2024 until November 2025 (https://portal.maap.eo.esa.int/earthcare/ec-baseline/, last access 13.3.2026). Dark orange indicated the period of reprocessing with Baseline BA.

2 Instrumentation and data products

2.1 ATLID's aerosol products

In this work, we analyze the performance of the ESA profiling products derived for ATLID, the high-spectral-resolution and polarization lidar operating at 355 nm. We focus on the geophysical quantities obtained from ATLID only, i.e., Level 2A products. Synergistic products, which also use other instruments of EarthCARE, are in the Level 2B product suite but are not in the focus of this work. To allow for synergistic products, all Level 2A products from the different instruments are calculated on a Joint Standard Grid with its respective product (X-JSG).

Notable changes in the ATLID product versions, partly based on updated calibration procedures, have taken place over the entire active mission lifetime and have influenced the product quality. Different product versions are called baselines and are named in 2 capital letters for the EarthCARE mission. It started with Baseline "AA" and when minor changes were included, the second letter was changed (e.g., to AB, AC, AD...). Major updates and software versions specifically aimed for data reprocessing of the entire database result in a change of the first letter and the reset of the second letter starting from "A" (e.g., BA, CA, DA...). Level 2A data, i.e., single-sensor data, have been publicly released in March 2025 with Baseline AE, while it was earlier available to official Cal/Val teams (Baseline AC was provided to them already in December 2024). For the first reprocessing of the entire data set with all algorithm updates since the start of the measurements, Baseline BA was rolled out in July 2025. This Baseline was used to reprocess the data set, so that one common set of data products is available from August 2024 to September 2025 to be comparable to each other. An overview of the baselines deployed for the ATLID profiling products which were available for validation teams is given in Fig. 2. A detailed description of what has changed between the different baselines can be found in the "EarthCARE product data handbook" at the disclaimer of each product (ESA, 2026).

Aerosol optical profiles, i.e., particle backscatter coefficient, particle extinction coefficient, and particle linear depolarization ratio from ATLID are calculated by A-PRO (ATLID-PROfile, Donovan et al., 2024) in the ESA product chain for EarthCARE. A-PRO provides different products (described below). These products depend not only on Level 1 data of ATLID (A-NOM, i.e., the attenuated backscatter coefficient profiles for the Rayleigh signal and the co- & cross-polar Mie signals), meteorological data (X-MET product) and the joint standard grid (X-JSG) but also on the outcome of the feature mask product, A-FM (van

Zadelhoff et al., 2023), to avoid averaging over strong and weak features together. While a full description of these product algorithms is beyond the scope of this work, we still want to summarize the main features and differences of the two profiling products in the following.

In the first profiling product, A-AER (ATLID - Aerosol), the aforementioned optical particle profiles are retrieved via the classical HSRL method. Guided by A-FM and other considerations (e.g. scattering ratio), a hybrid smoothing is performed on the three signals: Strong scattering features (like clouds) are smoothed less horizontally than weak scattering features (like aerosols). Based on the output of this procedure, a classical HSRL approach is applied along-track column-by-column to the horizontally smoothed signals providing fields of particle extinction and backscatter coefficient and particle lidar and depolarization ratio for aerosol and clouds. A simple multiple scattering (MS) correction is also applied. The two-dimensional fields of these products are then stored in the A-AER product file on X-JSG resolution, but one should remember that clouds are much less smoothed than aerosols regions. The main purpose of the A-AER product is to provide *a priori* information for A-EBD.

The second profiling product is A-EBD (ATLID Extinction, Backscatter, and Depolarization) and uses the same input as A-AER, i.e., A-NOM, X-MET, X-JSG, A-FM, but also the output of A-AER (including an initial target categorization). A-EBD applies an advanced optimal estimation (OE) scheme to optimize the extinction coefficient and the lidar ratio (and other variables) to fit the high-resolution observations (i.e. 1-km horizontal scale). The A-AER output, i.e., the lidar ratio, extinction but also the A-AER target classification are used as a starting point for the OE scheme (if available, otherwise default values are used). The geophysical products (backscatter, extinction, lidar and depolarization ratio of aerosol and clouds) are finally delivered at 3 different resolutions (low, medium, and high). The different resolution is, however, only applied to "weak" scattering features, e.g., aerosol targets, while strong scattering features are always supplied at high resolution. This means, e.g., that the low-resolution output of A-EBD is on X-JSG grid, but aerosol features are horizontally smoothed to 100 km while cloud features remain at high resolution (1 km). A multiple scattering correction is applied within the forward model of the OE scheme and is more accurate than the one applied in A-AER. Please note that within the A-EBD product, the lidar ratio is provided layer-wise and not in the same vertical resolution as the backscatter and extinction products. A-EBD also provides the final target categorization (A-TC) at the three different resolutions, but it is foreseen to provide only one resolution of this product in future. For most applications, A-EBD products are more accurate than the corresponding A-AER products and should be prioritized. We provided here only a brief description needed for the interpretation of the validation results, a detailed explanation of these products is given in Donovan et al. (2024).

In this paper, we focus on the analysis of the ATLID profiling products (i.e., A-AER, A-EBD) from Baselines B (i.e., BA and BB), but, whenever possible (e.g., in Sec. 3.2), we also show the changes introduced due to updated calibrations and processors with respect to earlier baselines, partly pre-operational and thus not provided to the public. All operational ATLID-only L2A processors (A-FM, A-PRO, A- LAY, van Zadelhoff et al., 2023; Donovan et al., 2024; Wandinger et al., 2023b) and their respective products have benefited from early Cal/Val activities and algorithm updates (e.g., Kubota et al., 2026). These activities will improve the synergistic L2B processors (and their products) as well, such as the synergistic products AM-COL (Haarig et al., 2023) using both, ATLID and MSI, or the ACM-CAP (Mason et al., 2023) making use of ATLID, MSI, and

Table 1. Overview of observational sites used for the validation of EarthCARE's ATLID profiling products based on golden case studies.

Name	Latitude	Longitude	Altitude	Geographical Area	Data availability
Mindelo, Cabo Verde	16.878°N	24.995 W	13 m asl	Outflow region of West Africa	since June 2021
Dushanbe, Tajikistan	38.559°N	68.856°E	864 m asl	Central Asia	since June 2019
Leipzig, Germany	51.353°N	12.435°E	125 m asl	Europe	since 2006
RV *Meteor*	3.940°N	35.295°W	5 m asl	Tropical Atlantic	26 Jan 2025
	10.849°N	22.262°W	5 m asl	Tropical Atlantic	6 Feb 2025
Invercargill, Aotearoa New Zealand	46.417°S	168.331°E	5 m asl	Southern Ocean	since August 2025

CPR, until the final radiation closure processors ACMB-DF (Barker et al., 2025) using all 4 instruments onboard EarthCARE. The algorithm updates include improved corrections (at levels 1 and 2) for radiation noise effects, a hot pixel correction, the removal of the 20-km spike feature, and improved depolarization ratio calculations, among many others (Donovan, 2025). Here, we focus on the performance of ATLID L2A profiling products of Baseline BA (BB) as is, without discussing the corrections themselves.

2.2 PollyXT and its data products

As ground-truth we utilize the measurements of the well-established PollyXT lidar systems (multiwavelength-Raman-polarization lidars, Engelmann et al., 2016) using tailored data products of the PollyNET (Baars et al., 2016) processing chain (Klamt et al., 2024). The lidar systems are part of the European research infrastructure for aerosol and clouds ACTRIS (Laj et al., 2024), and follow the quality assurance procedures of this infrastructure originally implemented in the framework of the European Research Lidar Network EARLINET (Pappalardo et al., 2014). To be ready for EarthCARE validation, these lidar systems took part in the preparation activities in the framework of an ATMO-ACCESS pilot project and proved their readiness already before the EarthCARE launch (Baars et al., 2024; Marinou et al., 2024). While the capabilities of the different systems slightly differ (Engelmann et al., 2016; Heese et al., 2025), and are continuously improved over time (Engelmann et al., 2025), all of the used PollyXT lidar systems operate at 3 wavelengths (355, 532, 1064 nm), have polarization and Raman capabilities, and a dedicated near-range telescope to also cover the lowermost atmosphere. As all systems are part of ACTRIS/EARLINET, they follow the standard operation and quality assurance procedures, e.g., telecover test and routine $\Delta 90°$calibrations for polarization observations (Freudenthaler, 2008; Wandinger et al., 2016; Freudenthaler, 2016; CARS, 2023a, b). Thus, the systems provide independent reference profiles of the particle backscatter coefficient, particle extinction coefficient, and particle depolarization ratio at (but not only) 355 nm – ATLID's operating wavelength.

2.3 Ground-based lidar stations

For the validation work, we utilize observations from PollyNET lidars at five different locations listed in Table 1 and shown in Fig. 1 to obtain a broad geographical coverage.

TROPOS operates permanent PollyNET lidar sites west of continental Africa at Mindelo (Cabo Verde), in Europe at Leipzig (Germany), and in Central Asia at Dushanbe (Tajikistan). Furthermore, we utilize measurements from two ACTRIS exploratory platforms hosting a PollyNET lidar, namely OCEANET and LACROS. OCEANET was operated on board the German research vessel *Meteor* in the Tropical Atlantic during voyage M207 (Hummels, 2025) in January and February 2025. LACROS started operating in Invergargill (Aotearoa New Zealand) in August 2025 as part of the goSouth-2 campaign (Seifert et al., 2025). A brief description of these sites is given in the following sections.

2.3.1 Mindelo, Cabo Verde

The ACTRIS supersite in Cabo Verde in the eastern Tropical Atlantic is located at Mindelo, on the island of São Vicente and is hosted by the Ocean Science Center Mindelo (OSCM). The aerosol conditions at Mindelo are typically characterized by the presence of geometrically and optically thick lofted layers of Saharan dust between June and September and a mixture of dust and biomass-burning aerosol between November and March. Cloud occurrence in the planetary boundary layer (PBL) below 2 km is very common, and cloud formation at the top of the dust layer can sometimes be observed (Gebauer et al., 2024, 2026).

2.3.2 Dushanbe, Tajikistan

The ACTRIS facility at Dushanbe in Tajikistan, Central Asia, is located at an altitude of 864 m above sea level. The facility is hosted by the National Academy of Science of Tajikistan. Like Cabo Verde, Dushanbe is also located within the global dust belt, frequently affected by both lofted and close-to-ground dust layers (Müller et al., 2025). Hofer et al. (2020a, b) showed that Dushanbe is not only influenced by dust from the classical deserts in Central Asia and beyond, but also by re-suspended salt and dust originating from numerous desiccating lakes (e.g., Aral Sea). Characterized by a continental climate, the site in Dushanbe can be described as hot and dry in summer, and cold and dry in winter.

2.3.3 Leipzig, Germany

Regular measurements in Leipzig, Germany, at the premises of the Leibniz Institute for Tropospheric Research, have been performed since 2000 as part of EARLINET (e.g., Mattis et al., 2004). In 2005, the first continuous observations with Polly lidars started. Leipzig is characterized by a humid continental temperate climate and meanwhile exposed to only low pollution levels. Nevertheless, frequent dust plumes from the Sahara are observed from spring to autumn above the local PBL. Recently, an increasing frequency of observations of smoke, mainly originating from North America, have been made. While some of these smoke plumes originated from pyrocumulonimbus activity, reaching therefore also the stratosphere and persisting for months (Baars et al., 2019), many smoke layers are observed in the free troposphere with several levels of intensity (e.g., Haarig et al., 2018; Gast et al., 2025).

2.3.4 OCEANET, ship-borne, Atlantic Ocean

At the beginning of 2025, a 5-week research voyage with the German Research Vessel *Meteor* took place in the Tropical Atlantic. On board was TROPOS' OCEANET facility, a sea-proof ACTRIS exploratory platform also operating a PollyXT lidar (Rittmeister et al., 2017; Bohlmann et al., 2018). The voyage started on 4 January in Belem, Brazil, and finally reached Mindelo, Cabo Verde, about 5 weeks later after studying the oceanographic and meteorological processes in the Tropical Atlantic, focusing on the western boundary circulation and long-term measurements of the Atlantic Meridional Overturning Circulation (GEOMAR, 2025a, b). Next to its primary science objectives, four direct rendezvous with EarthCARE were accomplished, for which the ship cruised along the EarthCARE ground-track for several hours centered around the exact overfly time (Hummels, 2025). The atmospheric conditions during these overpasses were complex, ranging from convective cloud cover with precipitation to fair weather cumuli conditions and cloud-free scenarios with smoke-dust plume occurrences. Two of these overpasses are analyzed in detail below.

2.3.5 LACROS, Invercargill/Waihōpai, Aotearoa New Zealand

On 22 August 2025, first light was emitted into the atmosphere above Invercargill/Waihōpai, Aotearoa New Zealand, by the PollyXT system installed within the mobile ACTRIS platform LACROS. The measurements are taken in cooperation with the MetService/Te Ratonga Tirorangi of Aotearoa New Zealand in the framework of the goSouth-2 campaign to investigate the clean Southern Ocean atmosphere, and also its vulnerability to aerosol advection from other sources, and are foreseen to run until 31 March 2027 (Seifert et al., 2025). In terms of aerosols, the region at the southern tip of Aotearoa New Zealand's South Island/Te Waipounamu is unique: it is one of the most unspoiled and yet still accessible regions in the world mainly influenced by marine emissions only. Occasionally, there are also episodes with dusty and anthropogenically polluted air when air masses approach from Australia.

3 Validation of ATLID Level 2 aerosol profiling products

Direct comparisons of the aerosol optical properties (backscatter and extinction coefficients, lidar and depolarization ratio at 355 nm) are being made between the ground-based reference PollyXT and ESA Level-2 profiling products of ATLID, namely the A-AER and A-EBD products (Donovan et al., 2024) at different resolutions for the full reprocessed data set with Baseline BA covering August 2024 to September 2025. Nevertheless, algorithm development continues constantly and thus, for the latest case (at Invercargill/Waihōpai, Aotearoa New Zealand) Baseline version BB is applied. However, changes from BA to BB are considered minor for A-AER and A-EBD products. We screened the co-located observations for overpasses in close vicinity (shortest distance between ground-site and EarthCARE ground track < 20 km for all except one case study) and appropriate atmospheric conditions to select seven case studies for a detailed discussion on the potentials and limitations of ATLID profiling products of Baselines B. The closest available profile from the respective ATLID product was then used for comparison. The selected case studies cover several predominant aerosol types, atmospheric conditions, and geographical regions to discuss

Table 2. Overview of the seven analyzed case studies.

Case/ Section	Observation Area	Date	Atmospheric characteristics	Consistency w. ATLID	Key Findings/Issues tackled
1 Sec. 3.1	Mindelo, Cabo Verde	1 June 2025	Pronounced Saharan dust layer over marine boundary layer, high aerosol load	Good	A-AER and A-EBD low-resolution products perform excellently within the SAL, except for overestimating the depolarization ratio outside the dust peak. In the marine BL, ATLID overestimates lidar ratio. Comparison of all profiling products.
2 Sec. 3.2	Dushanbe, Tajikistan	2 Sep 2024	Central Asian Dust trapped between high mountains, medium aerosol load	Good	Excellent overall agreement for Baseline BA, except for slight depolarization ratio overestimation. Improvements from Baseline AC to BA discussed.
3 Sec. 3.3	Leipzig, Germany	26 June 2025	Mixed dust and continental/marine aerosol in a complex heterogeneous environment	Problematic	Oscillations due to abug in the joint standard grid. Lidar ratios are too high due to disturbed A-AER retrieval reflected in the A-EBD backscatter and extinction values. Profile shape does qualitatively agree very well for all provided products, but depolarization ratios are not reliable in low backscatter signal regimes. Edge effects become visible as well as unrealistic low error estimates.
4 Sec. 3.4	Leipzig, Germany	5 July 2025	Continental aerosol and tropospheric smoke, spatially homogeneous conditions	Moderate	Backscatter and extinction are in fair agreement. Lidar ratio deviating below 1.8 km and partly show unrealistic values. Depolarization ratio affected by edge effects and partly overestimated but generally low.
5 Sec. 3.5.1	RV Meteor, Tropical Atlantic	26 Jan 2025	Tropical high-altitude Cirrus, perfect co-location, complex atm. conditions below 3.3 km	Good in Cirrus	In Cirrus: Agreement in terms of backscatter and depolarization ratio for BA. Significant improvement from Baseline AC to BA discussed for such strongly depolarizing targets. But edge effects appear with Baseline BA for Cirrus and aerosol layers. Error estimates partly too low.
6 Sec. 3.5.2	RV Meteor, Tropical Atlantic	6 Feb 2025	Smoke–dust mix from Africa up to 3 km above marine BL, daytime observations	Moderate	Extinction and backscatter profiles are similar for BA and AC and in perfect agreement to ground-based truth for lofted layer. Depolarization values are too high for such BA in moderately polarizing regimes.
7 Sec. 3.6	Southern Aotearoa New Zealand	24 Oct 2025	Pristine (AOD $\approx$ 0.03) but highly variable environment	Moderate	Medium- and high- resolution A-EBD products in excellent agreement for backscatter and extinction. Lidar ratios agree well except below 1 km where values are too low. Depolarization ratio products are not reliable in these pristine conditions.

a wide spectrum of EarthCARE capabilities. In the following, we investigate cases with mineral dust (Saharan dust at Cabo Verde and Central Asian dust at Dushanbe), marine aerosol (Cabo Verde), smoke (Leipzig), aerosol mixtures (Atlantic Ocean and Leipzig), cirrus (Atlantic Ocean), and clean background conditions (Aotearoa New Zealand) to cover almost all particle types listed in Wandinger et al. (2023a) and Floutsi et al. (2023). To guide the reader, the main features of the discussed case studies are summarized in Table 2.

3.1 Dust and marine aerosol at Mindelo, Cabo Verde

The first case study to be discussed targets the eastern Tropical Atlantic on 1 June 2025. Figure 3 shows an overview of the EarthCARE A-EBD products in this region. The "frame" (the name for the time-height section covered by EarthCARE) used is 05729A (i.e., the first segment of orbit 5729) and actually extends from 22.5°S, 17.2°W to 22.5°N, 25.9°W, covering 5064 km. However, only the region between 14.1°N and 19.7°N is shown in Fig. 3 to focus on the atmospheric conditions around the ground-reference site Mindelo, which is indicated on the maps as well as in the time-height plots of the ATLID products by a red vertical line. As seen on the zoomed-in map in Fig. 3, left, EarthCARE was very close to the Mindelo site, with a minimum distance of around 20 km. The particle backscatter coefficient, particle extinction coefficient, particle lidar ratio, and particle depolarization ratio (from top to bottom, respectively) measured by ATLID are shown in the right-side panels of Fig. 3. A pronounced dust layer (strong backscatter and extinction values indicated by yellow and reddish colors) at an altitude range from 1 to 6 km is visible in these products for the entire geographical region. The dust is characterized by a lidar ratio between 40 and 60 sr and an elevated particle depolarization ratio > 0.2, in agreement with many previous studies on the intensive properties of Saharan mineral dust (e.g., Floutsi et al., 2023; Haarig et al., 2022; Tesche et al., 2011; Freudenthaler et al., 2009; Groß et al., 2011; Veselovskii et al., 2016). Below the Saharan dust layer (or Saharan Air Layer – SAL), the marine boundary layer (BL) is visible, which was partly cloud-topped (white colors in the backscatter product). The marine boundary layer is usually characterized by lidar ratios below 30 sr and low depolarization ratio (Bohlmann et al., 2018; Haarig et al., 2017), which is in qualitative agreement with the lower lidar ratio values (bluish colors) measured by ATLID in this geometrically thin layer. Ice clouds are visible above 12 km, extending to 17.5°N. Due to their high variability, these clouds are not considered for comparison with the ground-site observations. In agreement with the EarthCARE observation, stable atmospheric conditions were observed at Mindelo below the cirrus level throughout the day, as indicated by the combined target classification (a combination of elastic only and elastic + Raman channels, Baars et al., 2017; Yin and Baars, 2021), shown in Fig. 4. The marine boundary layer, consisting of large, spherical particles, was present the whole day up to a height of about 1.2 km above ground (sea). On top of the marine BL, liquid clouds occasionally formed (bluish colors, e.g., at around 01 UTC). The dust layer, which was observed by EarthCARE (around 03:30 UTC in Fig. 3), was omnipresent the whole day over Mindelo, but faded out towards the end of the day, starting at 15 UTC. Broken high-altitude clouds (cirrus - indicated by greenish colors) were also observed throughout the day as partly seen by EarthCARE. Considering the temporal evolution of the atmospheric conditions over Mindelo as seen by ground-based lidar, together with the observed horizontal distribution seen by EarthCARE, we are extremely confident that the atmospheric conditions below cirrus level at Mindelo during the time of overpass have been representative for the EarthCARE aerosol profiles, taken with a minimum distance of 20 km away, even when considering the 100 km horizontal smoothing of the A-EBD low-resolution product. Such conditions make this case study ideal for evaluating the performance of ATLID L2A products, as representativeness issues, which usually exist in the validation of space-borne profiles (Amiridis et al., 2025; Floutsi et al., 2026), can be neglected for this case (and most of the following ones).

Figure 5 shows an overview of the ground-based profiles considered for the validation of EarthCARE. As PollyXT is a multiwavelength-Raman-polarization lidar, optical aerosol profiles can be acquired at several wavelengths. Even though in the

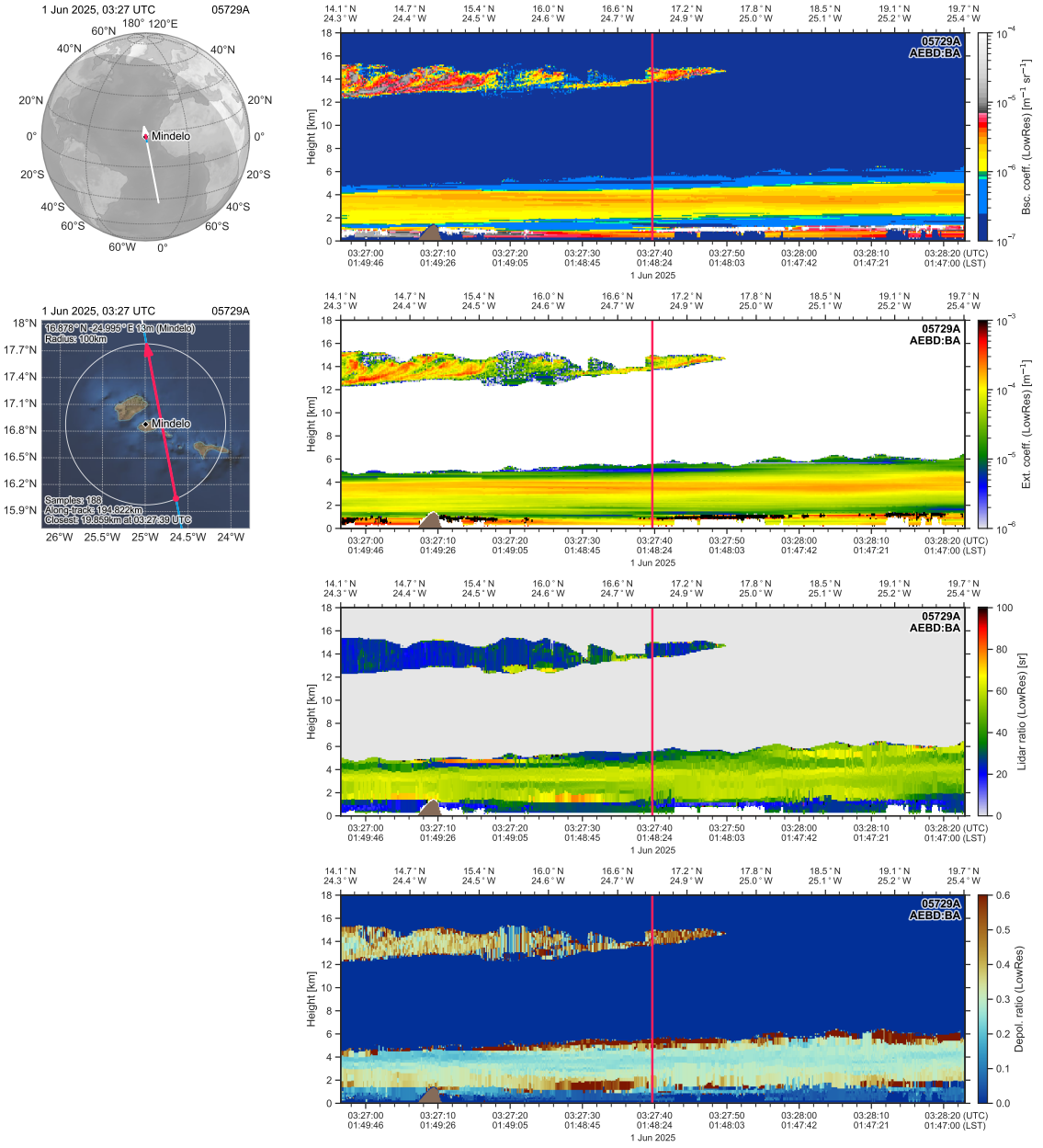

Figure 3. Overview of EarthCARE measurements around Cabo Verde on 1 June 2025. Left: Maps indicating the position of the ground-track and the location of the ground-based reference site. Right: Time-height plots of the A-EBD product at low resolution from top to bottom: Particle backscatter coefficient, particle extinction coefficient, particle lidar ratio and particle depolarization ratio. The frame number and baseline are indicated in each panel. The red vertical line marks the closest distance (19.9 km) to the ground-based station at Mindelo. Times are given in Coordinated Universal Time (UTC) and Local Solar Time (LST).

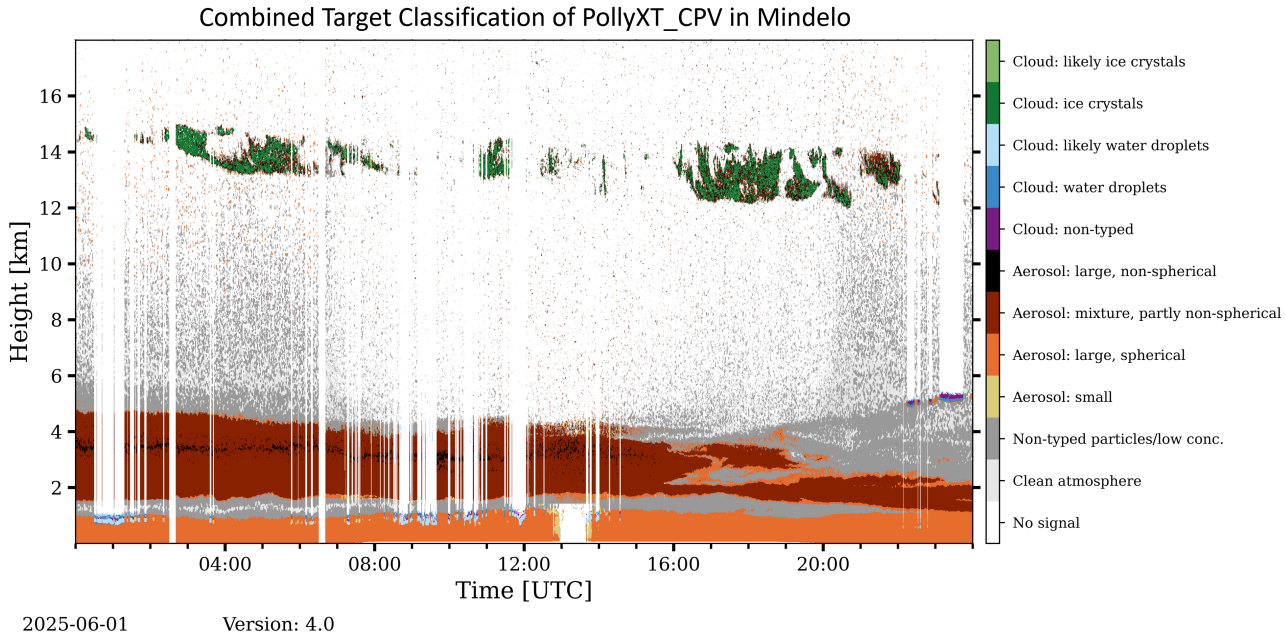

Figure 4. Combined PollyNET Target Classification (Hybrid approach, Baars et al., 2017; Yin and Baars, 2021) for Mindelo, Cabo Verde on 1 June 2025. Different aerosol and cloud types are classified according to the legend.

following we will concentrate on the ATLID wavelength of 355 nm only, we always evaluate the full spectral range available from the ground-based measurements to quality check the lidar performance itself, perform extended aerosol classification using the spectral dependence as additional information (Baars et al., 2017; Floutsi et al., 2024), and gather the intensive properties at all possible wavelengths to extend the collection of intensive properties for several aerosol types (DeLiAn, Floutsi et al., 2023). PollyXT has near-range capabilities using a second telescope. For the analysis of close-to-ground profiles, like the marine boundary layer in this case, we use the near-range profiles, while for the lofted aerosol layers or clouds, the far-range profiles are considered.

The observations shown in Fig. 5 for Mindelo on 1 June 2025 show the typical signature of a SAL above the marine BL. Wavelength-neutral backscatter and extinction (at 355 and 532 nm) values were observed for both aerosol layers of interest, while the 1064 nm backscatter is slightly lower (only about 80% of the 355 and 532 nm backscatter) in the dust layer. Marine aerosol and dust are characterized by large particles, which introduce little to no wavelength dependence. The marine and dust particles can be instead clearly separated by the depolarization ratio, which is close to 0 for marine particles and above 0.2 for dust particles (see the second panel to the right in Fig. 5). The lidar ratio values of about 60 sr at 355 nm in the SAL reveal slightly higher values compared to what is expected for pure dust, indicating slight pollution in this layer. In the marine boundary layer, lidar ratio values of around 20 sr were observed, thus indicating pristine conditions at Mindelo. All in all, the

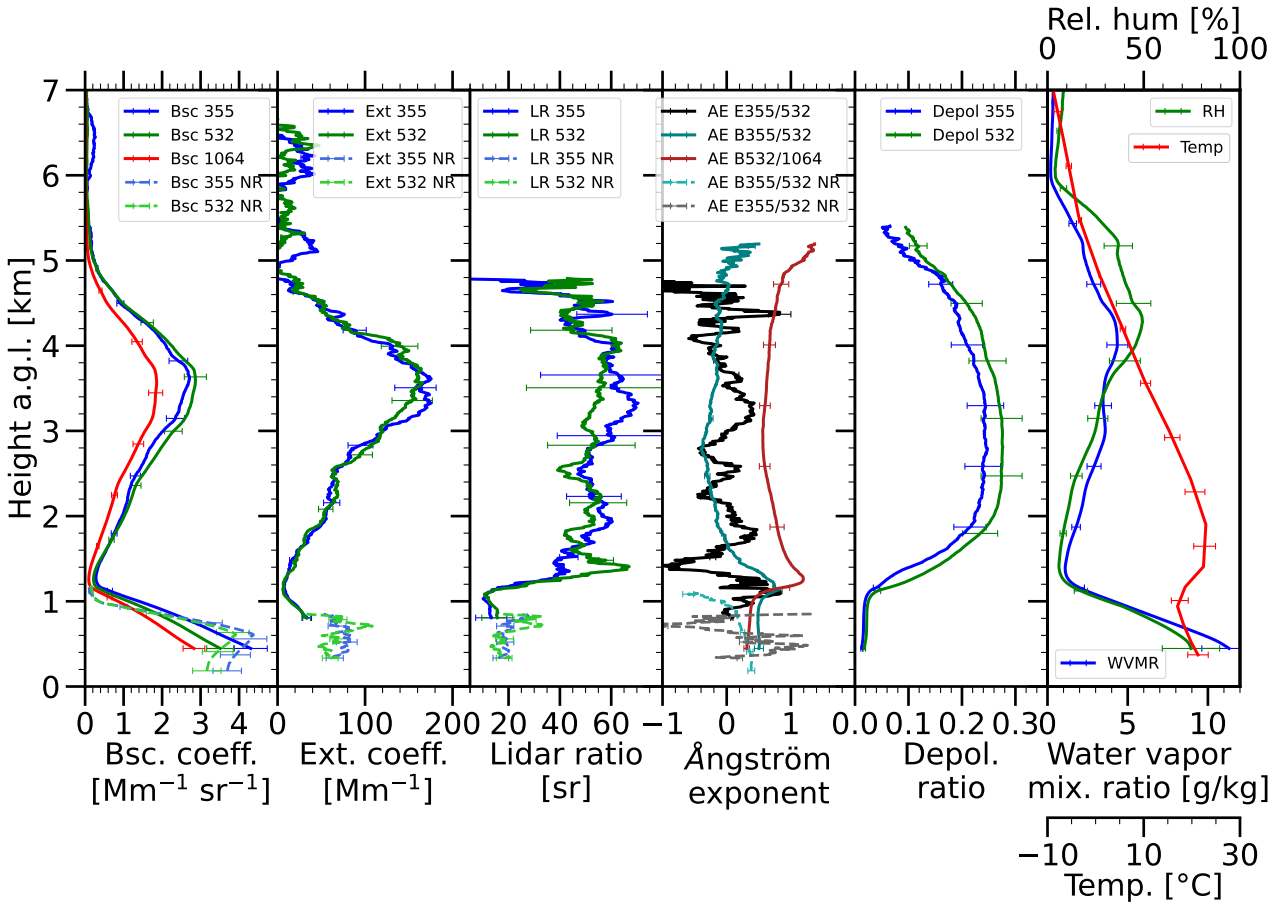

Figure 5. Vertical profiles of aerosol optical properties derived with the ground-based PollyXT lidar during the EarthCARE overpass at Mindelo on 1 June 2025 between 02:40 and 03:35 UTC. From left to right: Particle backscatter coefficient (Bsc), particle extinction coefficient (Ext), particle lidar ratio (LR), Ångström exponent (AE) with respect to backscatter and extinction as indicated in the legend, particle depolarization ratio (Depol), and water-vapour mixing ratio (WVMR). Products derived from the near-range receiver are shown additionally and are labeled explicitly with "NR". Furthermore, the temperature profile (Temp) derived from ECMWF IFS Analysis and short-term forecast is shown together with the relative humidity (RH) calculated from the lidar-derived water-vapour mixing ratio and the model temperature.

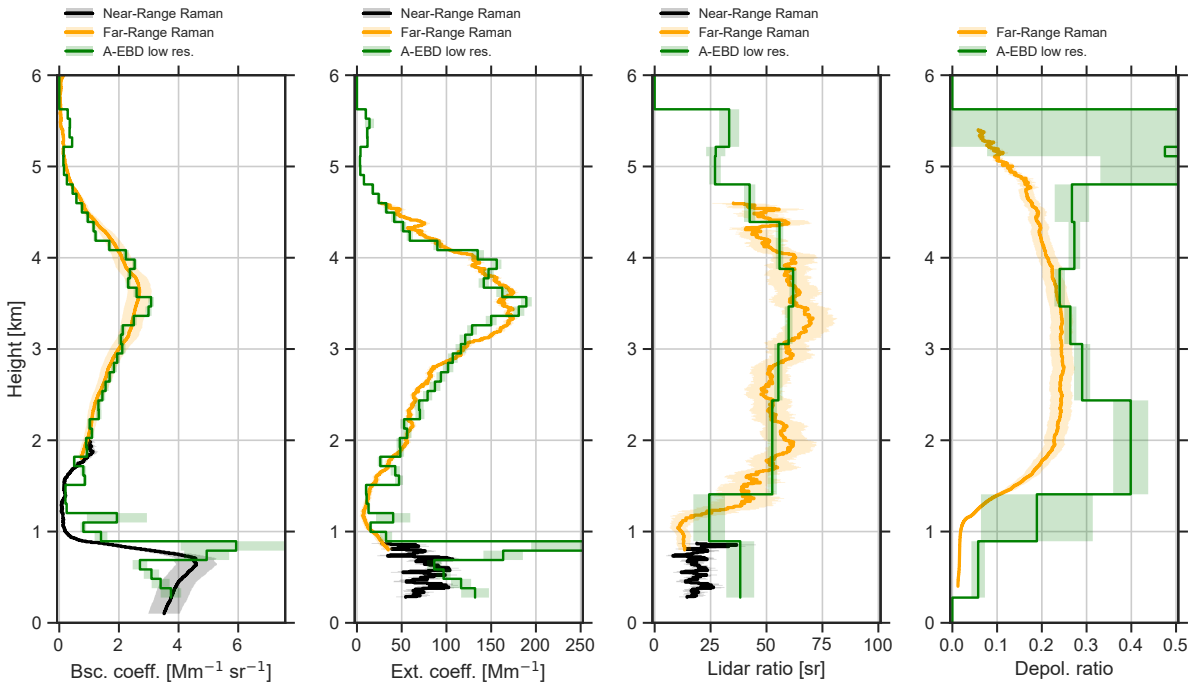

Figure 6. Comparison of EarthCARE A-EBD low-resolution products (Baseline BA) to ground-based PollyXT observations (averaged between 02:40 and 03:35 UTC) at Mindelo, Cabo Verde on 1 June 2025. From left to right: Particle backscatter coefficient, particle extinction coefficient, particle lidar ratio, and particle depolarization ratio.

derived optical properties provide a consistent picture of the atmospheric conditions on this day, with a clean marine boundary layer below 1 km and a partly polluted dust layer above, extending up to 5 km.

Figure 6 shows the direct comparison of particle backscatter and extinction coefficients, lidar ratio, and particle depolarization ratio between the ground-based reference and the respective EarthCARE A-EBD low-resolution profiles. Uncertainties are shown as shaded areas. An excellent agreement is found for the particle backscatter and extinction coefficient for the height region of 1.3 to 6 km, i.e., within the SAL. Within the marine BL (below 1 km height), these extensive quantities deviate slightly, most probably due to local differences in the lowermost atmosphere (e.g., cloud contamination).

Focusing on the aerosol intensive quantities, namely the particle lidar and depolarization ratio, one sees an excellent agreement of the lidar ratio in the SAL. Within the marine BL however, ATLID overestimates the lidar ratio with values of about 38 sr, which is clearly too high for pure marine particles (Floutsi et al., 2023). As shown in Fig. 3, marine conditions are expected at both measurement locations: at Mindelo, but also at the EarthCARE ground-track location, being 20 km east, directly above the ocean.

Regarding the particle depolarization ratio, excellent agreement is found in the height range of maximum dust load at 3.5 km altitude with values of 0.24. However, at regions with less dust load (lower backscatter) above and below 3.5 km, the retrieved

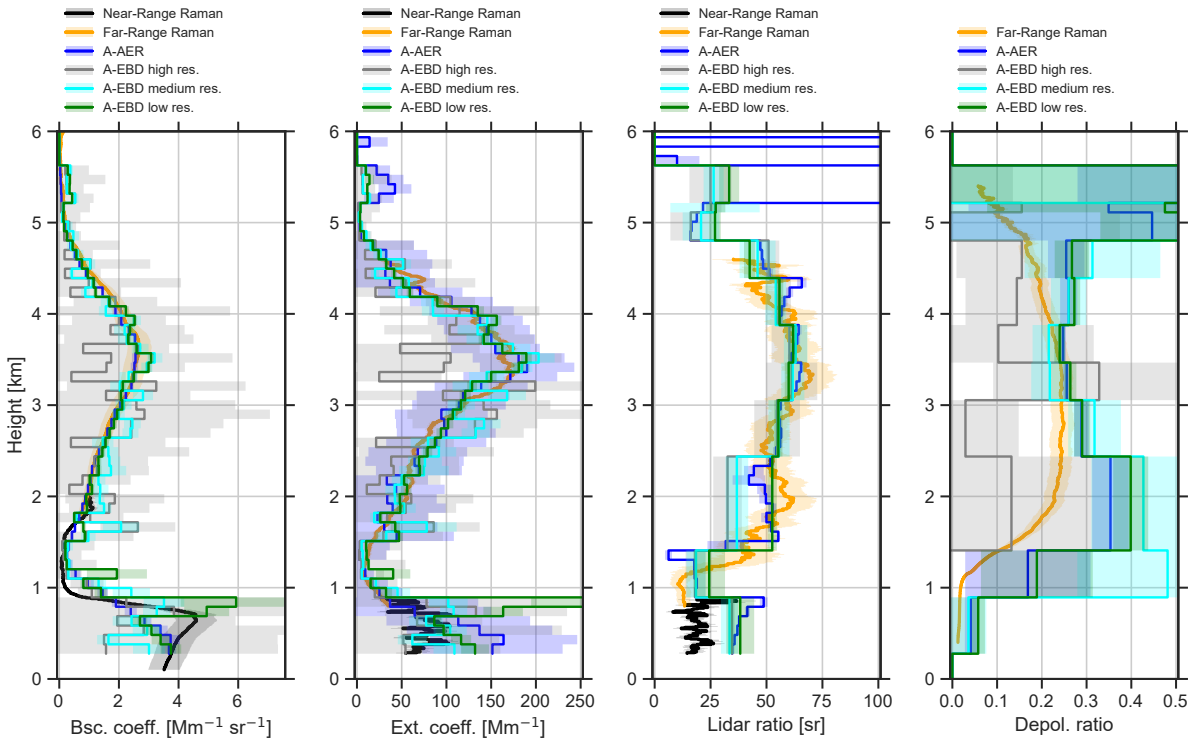

Figure 7. Same as Fig. 6 but for all A-EBD resolutions and A-AER (Baseline BA).

values deviate from the PollyXT profiles. Generally, A-EBD provides higher values (maximum of 0.4 at 2 km) than measured with the ground-based reference. Within the marine BL, A-EBD reports a depolarization value of 0.06, while PollyNET values are about 0.02.

Besides the A-EBD low-resolution products, there are three more products providing vertical profiles of aerosol properties from ATLID only, namely A-AER and A-EBD medium & high resolution. All of these products are shown together for illustration in Fig. 7. Here it becomes obvious that for these stable atmospheric conditions in the lofted aerosol layer, all products provide reasonable results besides the issues already discussed. However, as expected, the A-EBD high-resolution product is the noisiest product, having a large uncertainty and deviating partly from the reference values, but all still within the provided uncertainties. The A-EBD medium-resolution product becomes noisier when getting closer to the ground due to a decreasing signal-to-noise ratio while penetrating the dust layer. The lidar ratio values above 2.5 km, however, are interestingly accurate for all products (even for high resolution). Likely, this is an effect caused by the usage of the A-AER (lidar ratio) product as *a priori* for the optimal estimation in A-EBD. Below 2.5 km, the lidar ratios of the high and medium-resolution products start deviating and show values already close to marine conditions (about 25 sr) around 1 km asl. However, in the marine BL itself, the values are too high for all products as discussed previously.

Concerning the particle depolarization ratio in the SAL, it becomes obvious that the high-resolution product is not reliable for this parameter, with depolarization ratio values much lower than the reference and being noisier at the same time. The tendency of the medium-resolution product to get worse close to the ground is also evident in the particle depolarization ratio profile, while above 2.5 km, the values of medium- and low-resolution A-EBD and A-AER are similar. Nevertheless, the general and most obvious issues with respect to the particle depolarization ratio for weakly scattering targets as discussed above (significant deviation from the reference) remain for all four products and need to be tackled in new baseline versions in the future.

In summary, we can conclude that the A-AER and A-EBD low-resolution products perform well within the Saharan dust layer, except for overestimating the depolarization ratio. Efforts to improve the polarization ratio have been made since the beginning of the mission and are discussed further below (Sec. 3.2) and in a dedicated work (Haarig et al., 2025b), but still leave room for improvement. But generally, the excellent high-spectral-resolution lidar products, including the lidar ratio in the lofted aerosol layer, can be seen as a proof of concept for ATLID HSR profiling capabilities.

3.2 Dust in the high mountains at Dushanbe, Tajikistan

A second case study to be discussed is covering Frame 01508B on 2 Sep 2024. The ground-reference measurements were taken in Dushanbe, Tajikistan, in the eastern part of the dust belt (see Figure 1), and thus in a completely different geographical region than the first case study.

Figure 8 shows the corresponding products of ATLID (A-EBD low resolution) together with the local topography from 35.4°N to 41.6°N, centered around the overpass over Dushanbe at 21:04:35 UTC (nighttime). Minimum distance to the ground site was as low as 17 km. A remarkable dust layer trapped between the mountain ridges is seen in all four ATLID products. The dust layer is characterized by extinction values of about 50 Mm^{-1} (greenish/yellowish colors) to 200 Mm^{-1} (orange colors), with lidar ratios around 40 to 50 sr (green colors), and depolarization ratios of 0.15 to 0.3 (bluish colors). Occasionally, ice clouds are indicated by high depolarization ratios (red) at the top of the dust layer, e.g., around 37.8°N, but could also be an artifact as result of edge effects (discussed below). Interestingly, the top of the highest mountain ridges (above 4 km: Hindu Kush in Afghanistan at around 35.4°N and Zarafshan ridge at 39.1°N) seem to coincide with the top of the dust layer trapped between these ridges.

Atmospheric conditions over Dushanbe, as observed with the ground-based PollyNET lidar, were characterized by intense dust layers persistent for several hours to days. The derived optical profiles (geophysical parameters) from the PollyXT around the time of the EarthCARE overpass (2 September, 21 UTC, Fig. 9) reveal particle extinction coefficient values between 50 and 200 Mm^{-1} and thus indicate a medium aerosol load for this case study. The intensive optical properties, i.e., lidar ratio and depolarization ratio at all wavelengths (not shown), clearly indicate Central Asian dust (Hofer et al., 2017) as the main aerosol type in the lofted layer. Below 400 m above ground level (agl — 864 m offset to above sea level), a polluted planetary boundary layer was found, which will not be compared to EarthCARE products due to its shallowness and local occurrence. The direct comparison between the ground-based lidar observation and the closest EarthCARE A-EBD product at low resolution is shown in Fig. 9. Focusing on the main dust layer above 1.2 km altitude above sea level (asl) to 3.5 km asl, an excellent agreement is seen for the backscatter coefficient between ATLID A-EBD and the Raman retrieval of PollyXT. From 3.4 to 4.5 km, slight

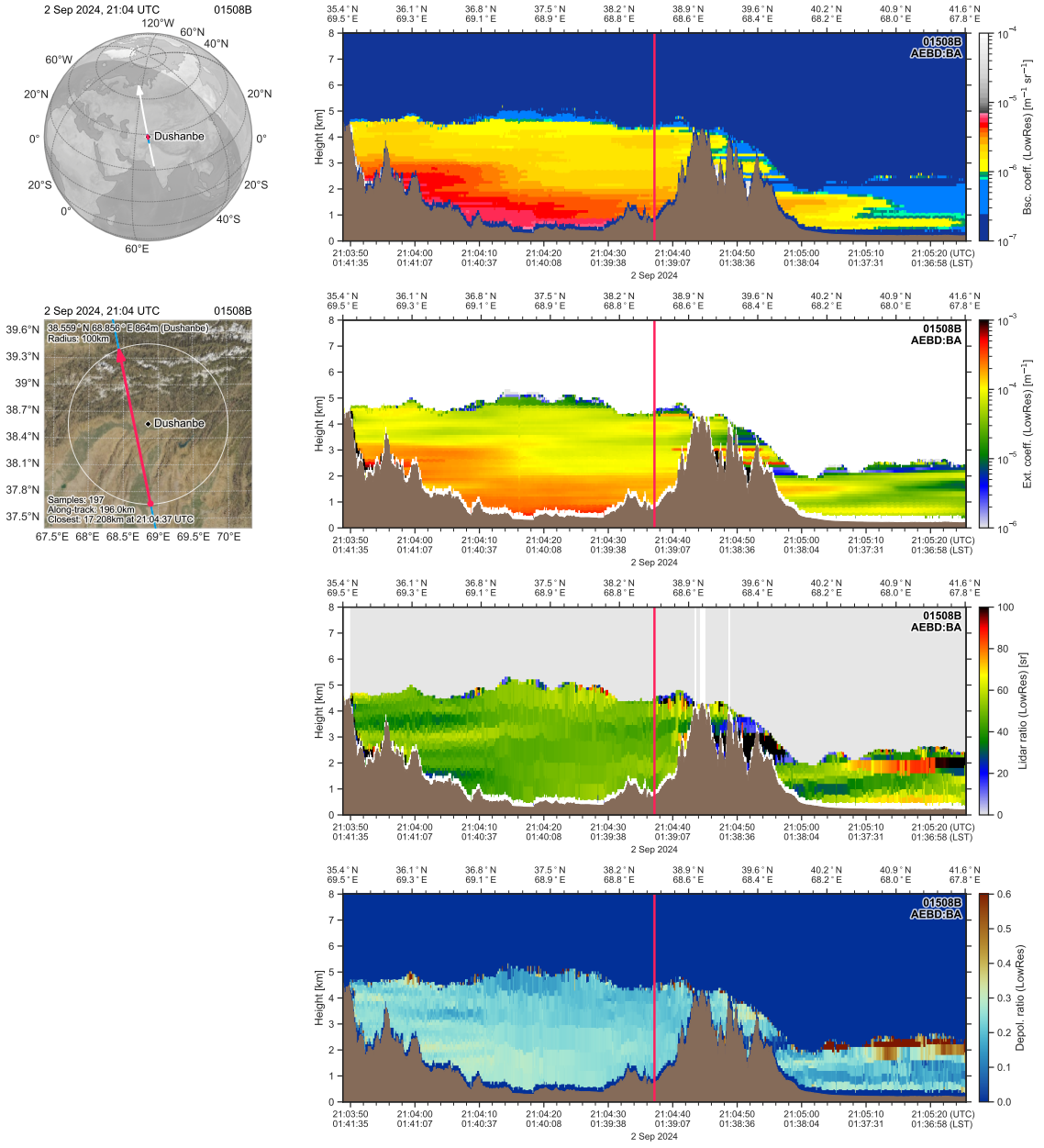

Figure 8. Same as Fig. 3, but for the overview of EarthCARE measurements around Dushanbe, Tajikistan on 2 Sep 2024. The red vertical line marks the closest distance (17.2 km) to the ground-based station at Dushanbe. Brownish colors indicate the local topography.

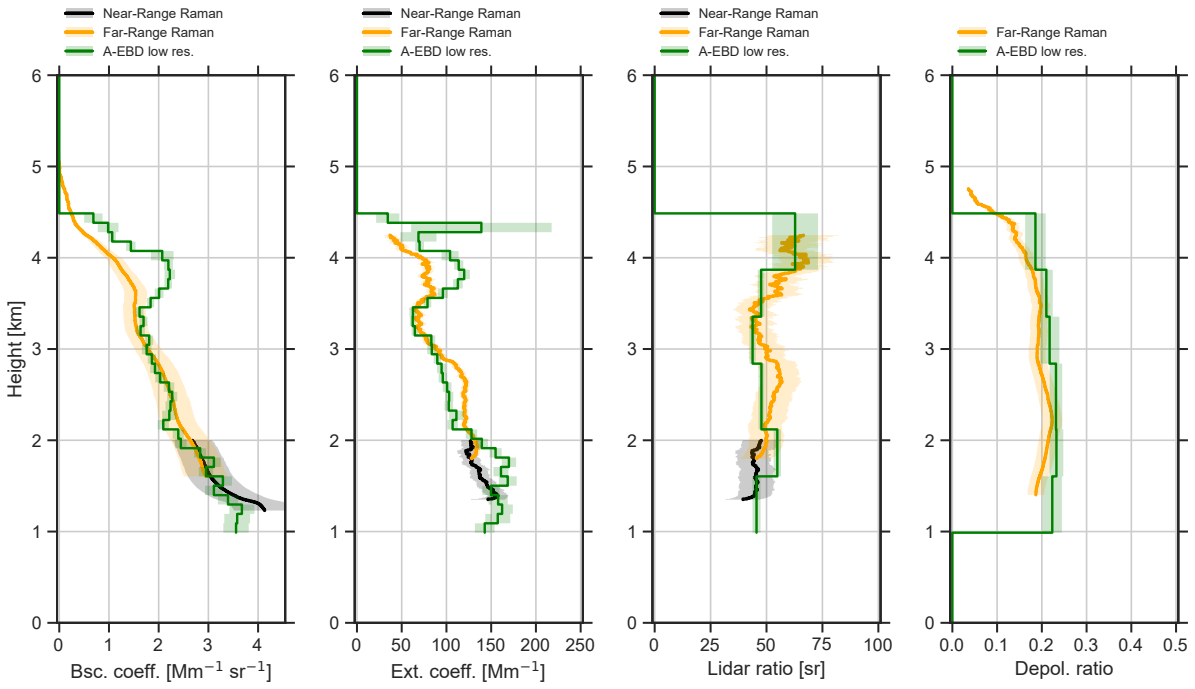

Figure 9. Comparison of EarthCARE A-EBD low-resolution products (Baseline BA) to ground-based PollyXT observations (averaged between 20:00 and 21:30 UTC) on 2 Sep 2024 at Dushanbe, Tajikistan. From left to right: Particle backscatter coefficient, particle extinction coefficient, particle lidar ratio, and particle depolarization ratio.

deviations become evident, which might be related to local heterogeneity in these uppermost layers. For the extinction, a good agreement is also found, but with some more fluctuations. Instead, the lidar ratio of A-EBD low resolution matches perfectly within the uncertainties of the two measurements. Both instruments measure lidar ratio values between 45 and 50 sr at 355 nm in this dust layer. Please remember that the lidar ratio of ATLID is provided layer-wise and not within the same resolution as the backscatter and extinction products, thus, larger steps are visible compared to the backscatter and extinction profiles of ATLID. For the depolarization ratio, the agreement is fair, but a systematic discrepancy characterized by a slight overestimation by ATLID is obvious. While the ground-based lidar measured depolarization ratios of 0.17 to 0.21, indicating slightly polluted dust, ATLID observed values of around 0.18 – 0.23, but always higher than the reference.

The early date of the case study in EarthCARE's lifetime also allows us to study the improvements/changes that have been implemented in the processing chain since the start of the mission. Fig. 10 shows the comparison for the same atmospheric scene, but as processed with the operational Baseline AC (at the very beginning of the mission) and compared to the reprocessed Baseline BA, which is the focus of this paper. A-AER (top panels) and A-EBD low-resolution products (bottom panels) are shown. From Baseline AC to BA, several improvements/modifications have been implemented in the processing chain to account for, e.g., hot/cold pixels, background correction issues, biases due to improper vertical smoothing (in A-AER), and

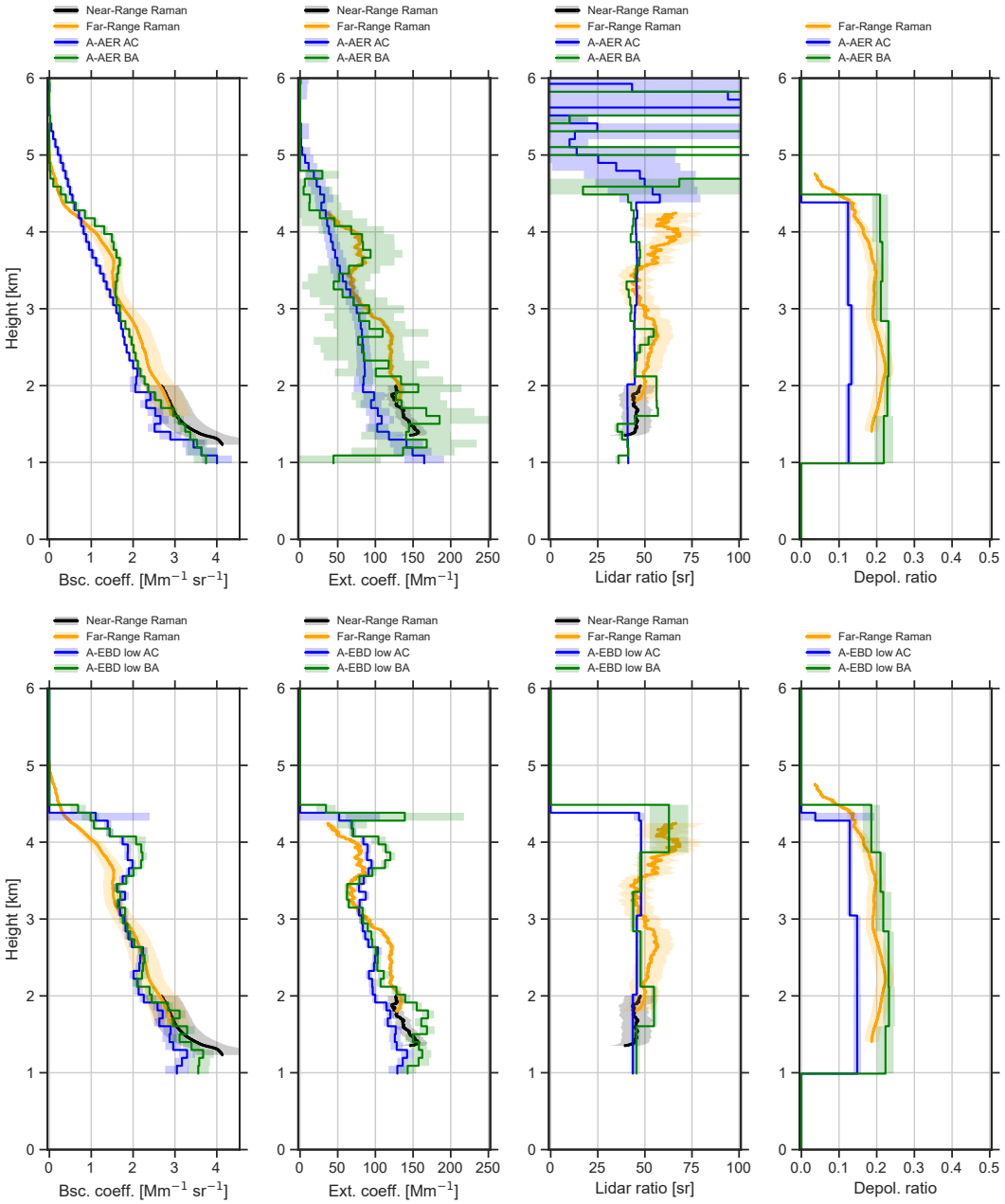

Figure 10. Same as Fig. 9, but for the comparison of Baseline AC (blue) and BA (green) for A-AER (top) and A-EBD low-resolution (bottom) products.

many more. The explanation of all these developments is beyond the scope of this work, which will focus on the results of the improvements only. Further details will be presented in dedicated publications, for example, improvements in the Level 1 data quality in general (Donovan, 2025) and in the depolarization ratio (Haarig et al., 2025b). With Fig. 10, we want to illustrate the overall effect of all these changes and to highlight the ongoing efforts for better data quality.

The most prominent change in EarthCARE data from Baseline AC to BA is observed with respect to the particle depolarization ratio for both products, A-AER and A-EBD. Here, too low values were reported in the beginning of the active mission (Haarig et al., 2025b; Gebauer et al., 2025). By introducing an improved background correction of the cross-polarized channel with Baseline AD and inserting the transmission coefficients measured in the pre-launch on-ground characterization with Baseline AE, the depolarization ratio has significantly improved. Now, the particle depolarization ratios are close to the ground truth, mostly overlapping within the measurement uncertainties of both systems. Other changes can be seen in the backscatter and extinction profiles, which result from several bug fixes (e.g., issues related to the screening of clouds when producing the medium and low-resolution optical property outputs). The values of backscatter and extinction have significantly increased (compared to Baseline AC) for the dust layer in A-AER and below 3 km altitude in A-EBD low resolution and are now (Baseline BA) much closer to the ground-truth. The lidar ratio values instead, have only changed slightly but mostly increased. The A-AER and A-EBD lidar ratio values have been already in the valid range (compared to the ground-truth) in Baseline AC. Now, the increase of the lidar ratio on top of the dust plume as identified with the ground-based PollyXT reference observations can be also reproduced with the A-EBD BA low-resolution product.

Concluding on this case of dust in Central Asia, we generally see an excellent agreement and an overall improvement of the ATLID products from Baseline AC to BA. The profiles in BA are now close to the ground truth, overlapping within the uncertainties, and thus give trust that the retrievals work well, at least for this specific case.

3.3 Dusty mix at Leipzig, Germany

The two cases discussed previously were measured in regions of the dust belt, where mineral dust plays the dominant role in the atmosphere. Now, we would like to discuss a case from Central Europe, namely Leipzig, Germany, to investigate the ATLID performance for a mix of dust with other aerosols, which occurred on 26 June 2025. The respective EarthCARE curtains are shown in Fig. 11. The atmospheric scene closest to Leipzig is again indicated by a red vertical line. On this day, an aerosol layer above the local PBL up to 6 km asl was observed by EarthCARE, coming from the Ore mountains in the south and flying over Leipzig towards northern Germany. The aerosol-layer-top height slightly decreased towards the north and the lofted layer itself obviously vanished around 52°N, thus 80 km north of Leipzig when only the local PBL remained. Backward trajectories and particle tracing simulations (Radenz et al., 2021b; Stein et al., 2015, not shown) indicate a clear pathway of air masses from the Saharan desert via the Iberian Peninsula towards the Atlantic and the North Sea before entering the continent towards Leipzig. Therefore, an uptake of marine aerosol and continental pollution, in addition to the mineral dust, is very likely. In the respective A-EBD products, some oscillations are seen (most prominent in the extinction plot, second panel in Fig. 11), which are not gravity waves nor other atmospheric features, but caused by a bug related to the joint standard grid of the EarthCARE

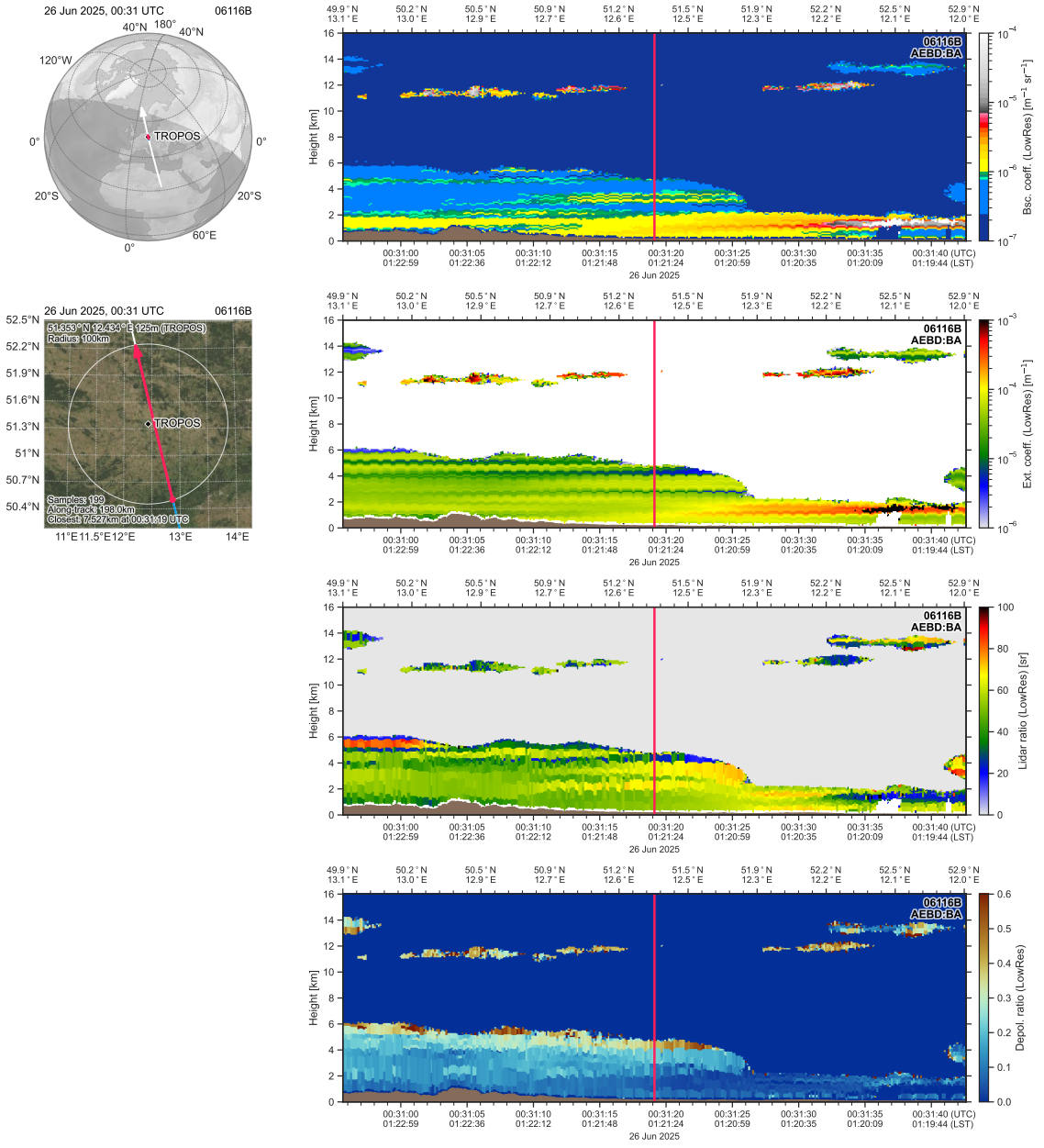

Figure 11. Same as Fig. 3, but for the overview of EarthCARE measurements on 26 June 2025 around Leipzig, Germany. The red vertical line marks the closest distance (7.5 km) to the ground-based station.

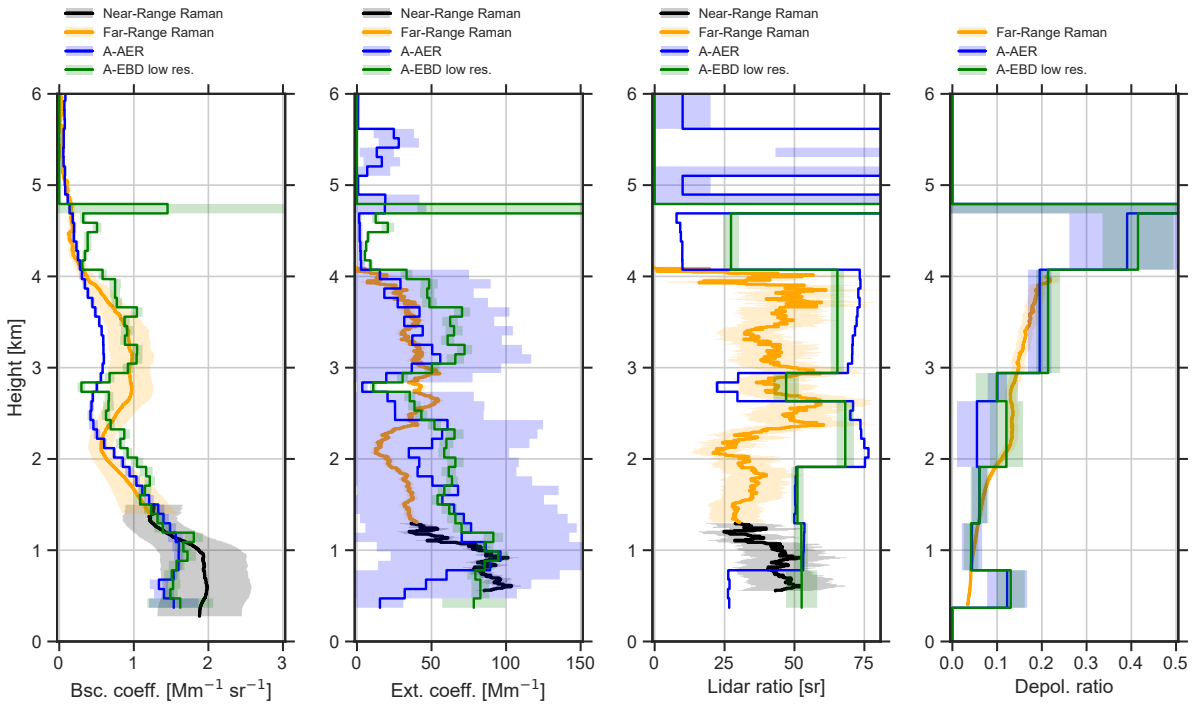

Figure 12. Comparison of EarthCARE A-EBD low-resolution (green) and A-AER (blue) products (Baseline BA) to ground-based PollyXT observations (orange, averaged between 23:45 UTC on 25 June and 01:15 UTC on 26 June) at Leipzig, Germany for the overpass on 26 June 2025, 00:31 UTC. From left to right: Particle backscatter coefficient, particle extinction coefficient, particle lidar ratio, and particle depolarization ratio.

processing chain, which shifts the height array from time to time by one bin. Nevertheless, the optical properties are not affected by this issue and thus do not hinder their analysis.

Fig. 12 shows the comparison of the closest ATLID profiles (7.5 km away, A-EBD low resolution in green and A-AER in blue) and the ground-based optical profiles retrieved from Polly. A nearly perfect agreement for this case in terms of the particle backscatter coefficient can be found between 1 and 5 km for the A-EBD low-resolution product. The extinction coefficient, however, appears to be overestimated by A-EBD except for the height region close to the ground (< 1 km) and between 2.5 to 3 km. This is also reflected in the lidar ratio profiles, which are generally higher than the ground-truth (around 50 to 75 sr for ATLID compared to 30 to 50 sr for the ground reference) in the pronounced aerosol regions. The higher lidar ratio values are caused by the A-AER results (shown in Fig. 12 as blue line) which serve as input to the optimal estimation in A-EBD. Dedicated investigations performed for this study in the framework of DISC (EarthCARE Data Innovation & Science Cluster) have shown that one erroneous A-NOM profile in the smoothing procedure of A-AER has led to unrealistic error estimates within the lidar ratio retrieval allowing for too high lidar ratio values. In addition, a very complex atmospheric layering with a strong spatial inhomogeneity occurred within the 100 km around Leipzig. As nicely seen in Fig. 11, a dust

layer (characterized by high depolarization ratio values) was situated around Leipzig and was partly on top of the existing near-surface layer of continental/marine aerosol (low depolarization ratio and moderate lidar ratio). During the time of the overpass, the northernmost edge of this dust layer was just 50 km away from Leipzig. But one has to remember that the horizontal averaging of the A-AER products is adaptive and can be as large as 100 km and, therefore, also includes regions more far away from the ground-based reference site than its closest distance. For these reasons, it is very likely that the complex layering together with erroneous profile reported previously, might have disturbed the A-AER retrieval and finally caused the overestimated lidar ratio values. Currently, studies on the root cause of the one erroneous profile within the 100 km around Leipzig are going on as well as investigations on how to flag such invalid profiles properly in future. The main take-home message with respect to the extinction and lidar ratio profiles is that, even though EarthCARE data is public, the data products of Baseline BA are not yet 100% quality assured and occasional errors in the retrieval can occur which are not yet properly flagged.

Besides the issue of the extinction and lidar ratio, for the particle depolarization ratio, we see an amazing agreement between the two lidars. The almost linear increase from ground (more pollution than dust) to higher values at the top of the aerosol layer (highest values of around 0.2 for the Polly observations indicating a mixture of dust with other aerosols) is also shown by the EarthCARE products. However, the increasing trend continues with height in A-EBD which cannot be confirmed by the ground-truth instrument. As discussed above, the air mass transport analysis indicated a clear transport pathway from the western Sahara towards Leipzig with a high probability of mixing with other aerosols, and thus confirming the findings of the ground-based reference. But even in the case of pure dust, values of the depolarization ratio of almost 0.40, as measured between 4 and 5 km by EarthCARE, are clearly overestimated in this atmospheric region with low scattering (low aerosol load) as dust depolarization ratios at 355 nm are usually well below 0.30 (Floutsi et al., 2023). Thus, obviously, the depolarization measurements of EarthCARE are not yet fully reliable in such aerosol regimes with low backscatter signal.

3.4 Continental aerosol and smoke around Leipzig, Germany

Another case of interest from Leipzig for the validation is 5 July 2025. Here, the EarthCARE overpass occurred about 75 km away from TROPOS. However, as seen in the cross sections in Fig. 13, a spatially very homogeneous aerosol layer was measured below 3 km around the overpass, allowing us to use this case for validation as well. The multiwavelength lidar observations at Leipzig indicate the presence of smoke from fires in North America throughout the troposphere which is also confirmed by backward trajectory (Radenz et al., 2021b; Stein et al., 2015) and model analysis (e.g., Peuch et al., 2022). Above the tropospheric aerosol layers, stratospheric smoke was observed by ATLID at around 11 km indicated by enhanced depolarization values and high lidar ratio values (>60 sr). The presence of smoke at this altitude was also confirmed by observations with the fluorescence lidar MARTHA (Gast et al., 2025) at Leipzig showing clearly enhanced fluorescence capacity values as typically for smoke (Gast et al., 2026). Interestingly, it seems to be that ice formation is triggered at the bottom of the smoke layer in some regions indicated by the very low lidar ratio. Nevertheless, to not lose focus, we concentrate on the tropospheric features below 6 km in the following.

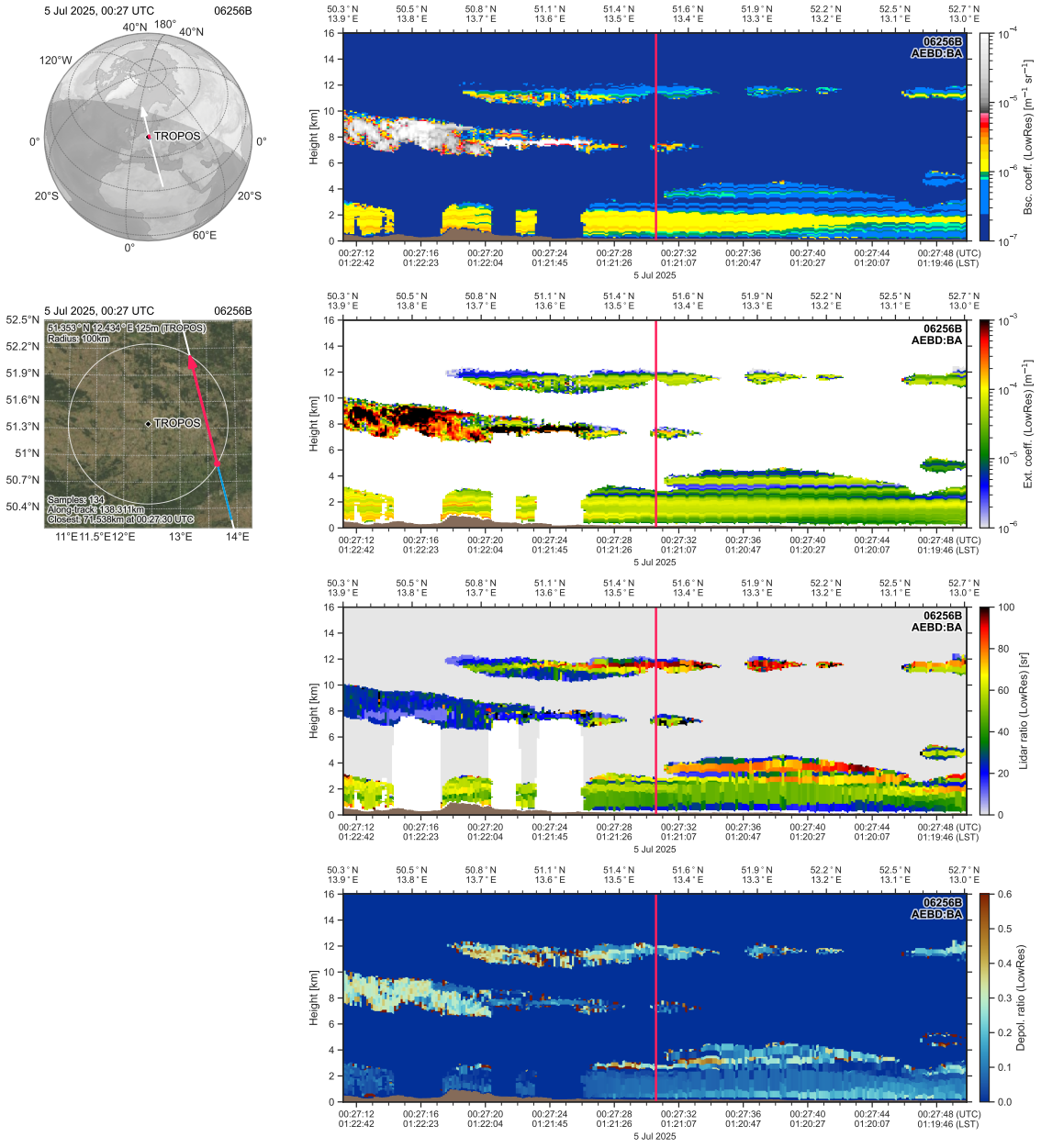

Figure 13. Same as Fig. 3, but for the overview of EarthCARE measurements around Leipzig, Germany on 5 July 2025. The red vertical line marks the closest distance (72 km) to the ground-based station.

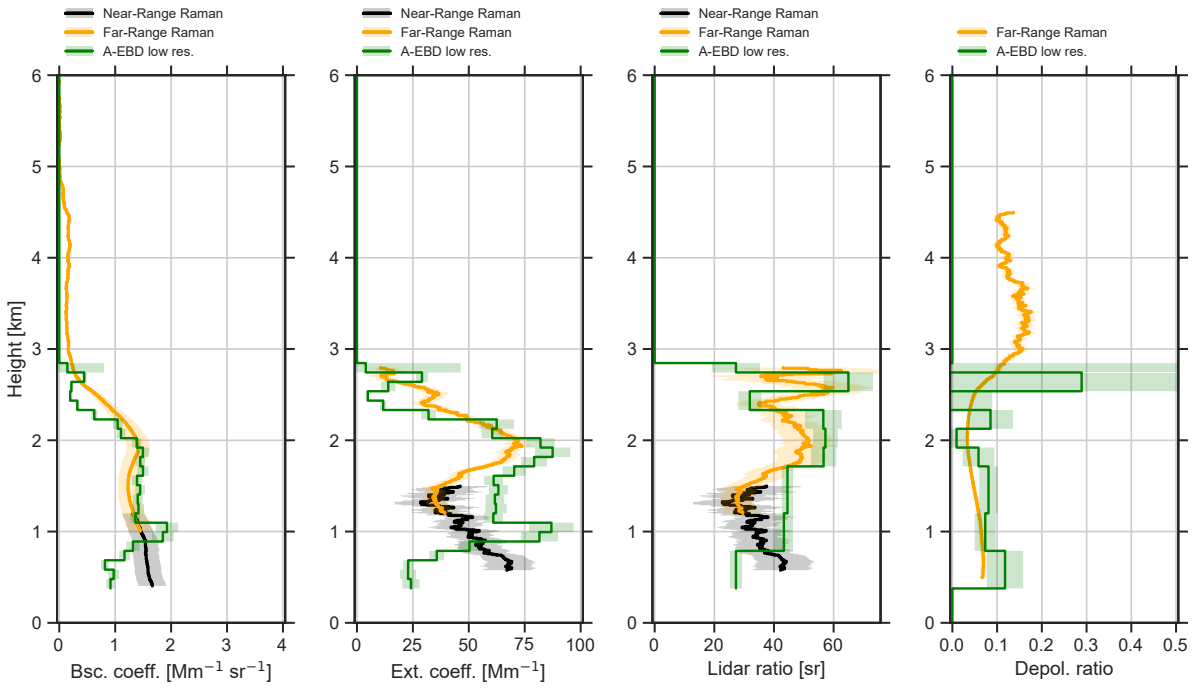

Figure 14. Comparison of EarthCARE A-EBD low-resolution products (Baseline BA) to ground-based PollyXT observations (averaged between 23:55 UTC on 4 July and 00:40 UTC on 5 July 2025) at Leipzig, Germany. From left to right: Particle backscatter coefficient, particle extinction coefficient, particle lidar ratio, and particle depolarization ratio.

The comparison of the ground-based optical profiles at 355 nm and the respective EarthCARE profiles are shown in Fig. 14. Despite the distance of the two observations, a very good agreement is found for the extensive quantity particle backscatter coefficient between 1 and 3 km altitude. Below, variations occur which can be explained with spatial inhomogeneity. The extinction coefficient is slightly overestimated below 2 km. The lidar ratio profile is in fair agreement (within the uncertainties) from 1.8 to 2.8 km, but overestimated from 0.8 to 1.8 km. Below 800 m, the A-EBD lidar ratio converges towards values below 30 sr, which cannot be confirmed by the ground-based PollyXT with its near-range capabilities (observing values above 40 sr in the BL below 1 km). However, considering the distance between the two observations of 75 km, not too many conclusions should be drawn for the comparison within the surface-near first 800 m, that are likely partially influenced by local planetary boundary layer processes in the summertime continental environment. Nevertheless, it still seems a bit suspicious that lidar ratio values close to clean marine conditions are provided by ATLID in this low altitude range. In contrast to the cases before, the aerosol conditions were dominated by spherical particles (continental pollution/smoke). Therefore, only low depolarization ratio values were observed by both instruments as indicated in the right panel of Fig. 14. Here, we see that the depolarization values of the reference measurements of PollyXT are lower compared to the values provided by ATLID. Between 1 and 2 km height, the mean particle depolarization ratio of PollyXT is 0.06–0.07, while A-EBD provides values of around 0.10. On the

top of the aerosol layer at around 2.7 km, A-EBD provides significantly too high depolarization ratio values which are most probably a result of edge effects (i.e., smoothing over the sharp boundary between the aerosol layer and the cleaner atmosphere above). However, also the given error for this value is very high so that the two profiles agree within their uncertainty range. Nevertheless, ATLID's profiling product should obviously not be used when such a large error range is given, spanning basically all possible values (in the case of the depolarization ratio from 0 to 1). Potentially, data should therefore be flagged as invalid in future.

We can conclude from this case that for aerosol conditions with low particle depolarization, EarthCARE's depolarization ratio products still need to be improved even though the absolute deviations are comparable low (when the respective uncertainties are low).

3.5 Aerosol and ice clouds over the tropical Atlantic observed on board RV *Meteor*

In addition to the observations made on land, we also had the opportunity for four direct overpasses during a research voyage with the RV *Meteor* on the Tropical Atlantic Ocean in Jan/Feb 2025 (see Fig. 1 and Hummels, 2025). While for two of these overpasses, atmospheric conditions were inappropriate for a direct comparison, we can utilize the rare opportunity for validating ATLID above the Tropical Atlantic for the other 2 cases.

3.5.1 RV *Meteor*: Cirrus

The first case to be discussed was measured on 26 January 2025. The respective cross sections of the A-EBD low-resolution products over the western Tropical Atlantic close to Brazil are shown in Fig. 15. Complex aerosol layering occurred below 5 km with occasional cloud formation in the regions around the overpass indicated by the red vertical line. Prominent features in these time-height plots (especially for extinction coefficient) are stratospheric layers between 18 and 26 km originating from the Ruang eruption (e.g., Khaykin et al., 2026). However, inconsistencies with sharp edges (see, e.g., lidar ratio plot) can be seen in this stratospheric layer. The detection of stratospheric features has not been a mission goal yet and, thus, it should be noted that the stratospheric retrievals are much less developed than the tropospheric ones (see, e.g., Wandinger et al., 2023a, Sec. 9). But further work with respect to stratospheric aerosol products is already envisaged.

More in focus of interest are the ice clouds at around 15 km altitude, which were persistently observed by ATLID and which are getting more intense towards the North. Due to the low-level-cloud contamination in the ATLID and PollyXT profiles, we will focus in the following mainly on this ice cloud layer. Because the lidar operated aboard RV *Meteor* (PollyXT OCEANET) is designed to retrieve extinction in the lowermost troposphere, direct extinction measurements in the vicinity of the ice clouds were not possible, and therefore we use the backscatter and depolarization measurements only. Also, the stratospheric layer cannot be analyzed with the PollyXT observations, as the signatures are too faint for this tropospheric lidar, especially as the signals were further attenuated by the ice cloud. Fig. 16 shows the comparison between ATLID (Baseline BA in green and Baseline AC in blue) and PollyXT. Despite the good collocation in space (within 400 m) and time (continuous cirrus coverage), the analysis of extensive properties, i.e., the backscatter coefficient, already reveals differences in the cirrus between ATLID and PollyXT observations. It should be noted, however, that a vertical smoothing of 750 m was applied to the PollyXT observations,

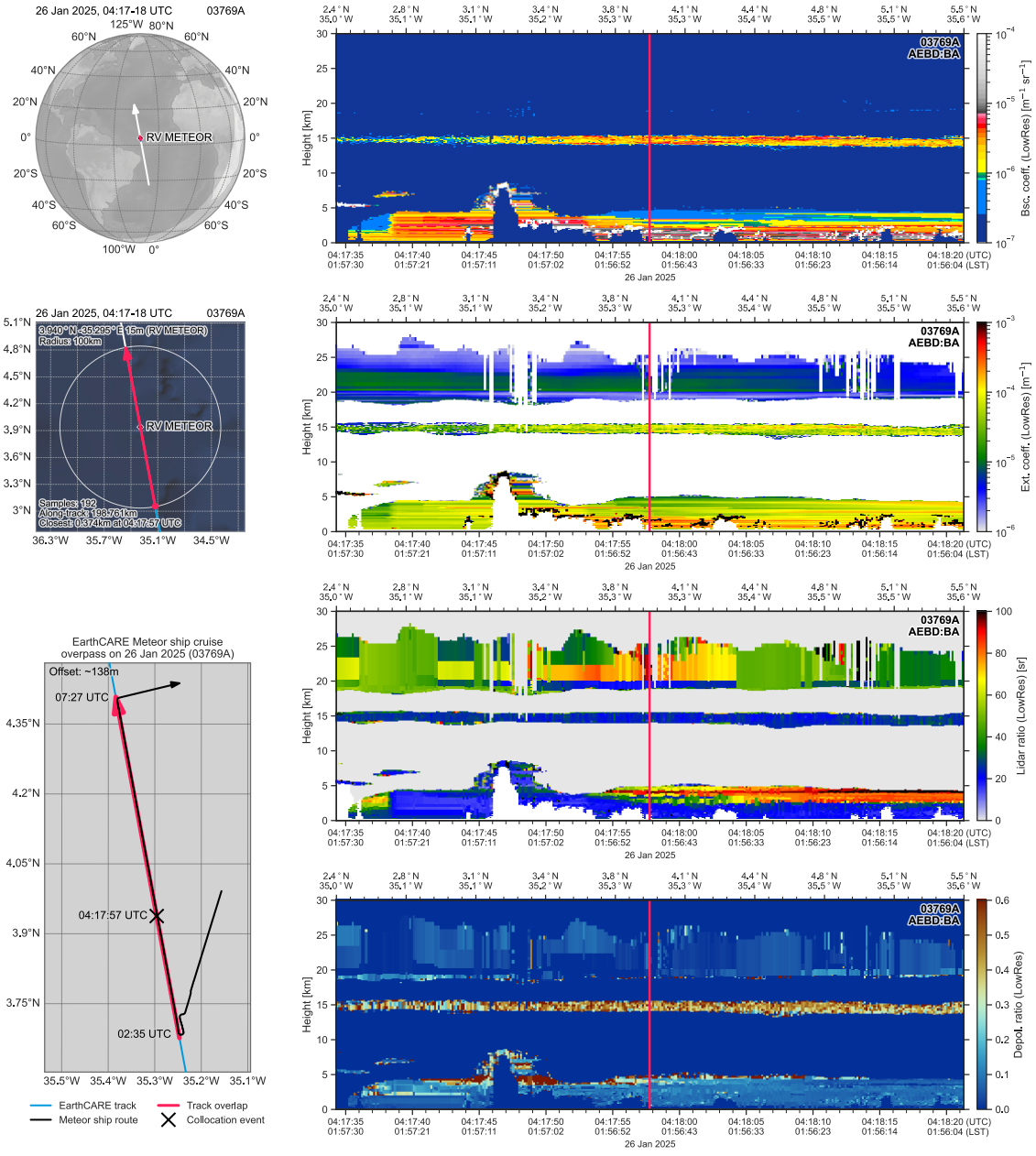

Figure 15. Same as Fig. 3, but for the overview of EarthCARE measurements on the Tropical Atlantic near 4°N, 35°W on 26 January 2025 (exact coordinates are given in the maps). The red vertical line marks the closest distance (0.375 km) to the Research Vessel *Meteor* during the overpass. The ship track and exact point of the overpass is also indicated in the lower, left panel. The given offset refers to the average absolute distance between the ATLID ground-track and the Meteor track (along the overlap, i.e., between 02:35 and 07:27 UTC).

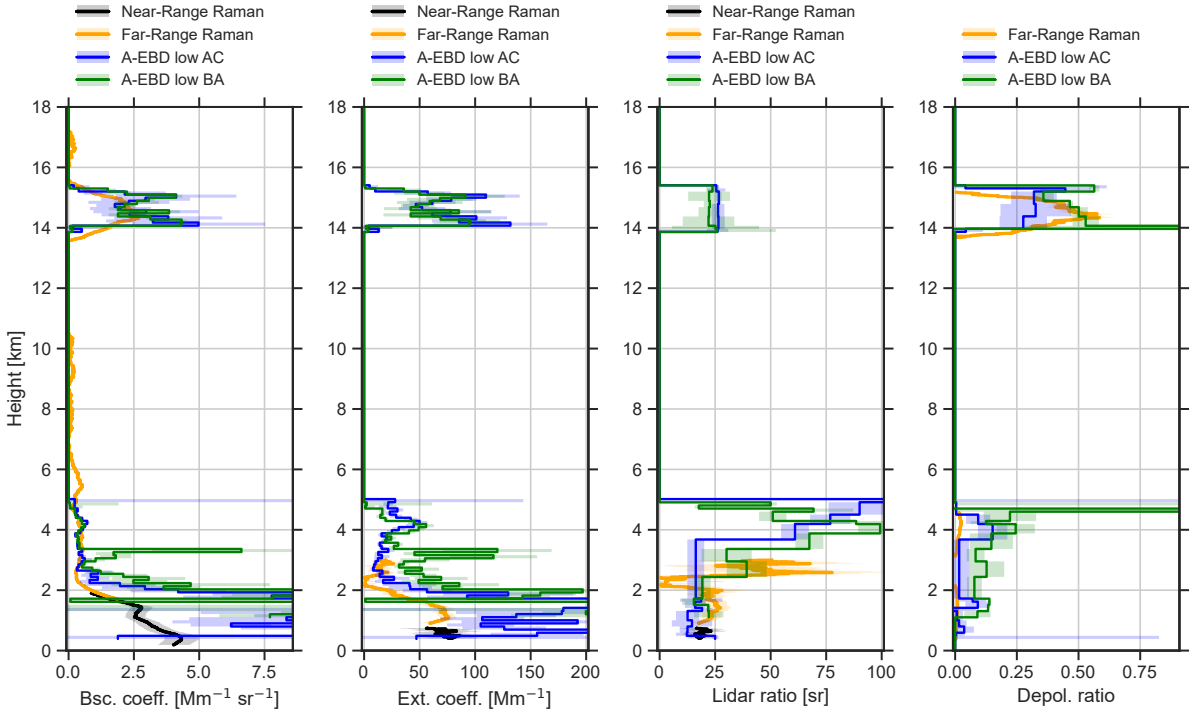

Figure 16. Comparison of EarthCARE A-EBD low-resolution products (Baseline BA) to ground-based PollyXT observations (04:30 UTC to 04:40 UTC) on board RV *Meteor* in the Tropical Atlantic on 26 January 2025. A-EBD products of Baseline BA (green) and Baseline AC (blue) are shown.

whereas ATLID retains its native vertical resolution of 100 m. For this reason, we can consider a fair agreement between the two observations in the cirrus region allowing us to have a look at the intensive particle property depolarization ratio. In the lower atmosphere below 5 km, the sporadic cloud occurrence makes any meaningful comparison impossible. Nevertheless, all values are still shown for completeness.

Concerning the particle depolarization ratio in the cirrus region, we see an excellent agreement for Baseline BA, with values of around 0.45–0.50 measured by both systems, except for the cirrus cloud bottom (unrealistically high values of more than 0.8) and top (spike in depolarization ratio values of ATLID). These findings indicate, as discussed in the previous case, that edge effects at the boundary of aerosol or cloud layers can occur and result in erroneous values in the A-EBD products. These unrealistic values can only partly be identified by the uncertainties provided: A high uncertainty of the depolarization value is provided at the bottom spike (at 14 km) while only a very low uncertainty is given for the value at the top spike (at ca. 15.5 km). It is worth to mention that PollyXT measures under 5° off-zenith and ATLID measures 3° off-nadir to avoid specular reflections which are, however, unlikely for cirrus cloud particles that formed at the temperatures of this event.

Comparing the results of the particle depolarization ratio to Baseline AC, one sees a significant improvement for this strongly depolarizing target, leading to the conclusion that for nighttime measurements of ice clouds, ATLID can already provide

meaningful and correct particle depolarization ratio values with Baseline BA. Interestingly, the unrealistic peaks at cloud bottom and top (edge effect) did not occur in Baseline AC, which needs further investigations with respect to the updates made in the A-EBD retrievals between the two baselines. Comparing Baseline AC and BA for backscatter and extinction, one sees almost no difference for the cirrus region. Consequently, only small changes are identified between Baseline BA and AC for the lidar ratio values in the cirrus region. But due to the missing ground-based reference profile, it is difficult to conclude further. We only can state that both baselines provided lidar ratio values in the realistic range for ice particles (Irbah et al., 2023).

Below ca. 3.3 km agl, increased backscatter and extinction values compared to PollyXT were observed, exactly in the atmospheric regions where the lower clouds occurred (Fig. 17). Thus, cloud contamination is very likely and makes a meaningful comparison impossible. However, we also identify edge effects occurring in the profiles of lidar ratio (values up to 100 sr) and depolarization ratio (values close to 1) at the top of the aerosol layer at around 4 to 5 km.

3.5.2 RV *Meteor*: Smoke-dust mix

The second validation case from the RV *Meteor* voyage was collected on 6 February 2025. The ship was located in the eastern Tropical Atlantic and EarthCARE overpassed it at 15:33 UTC as can be seen in Fig. 17. During this overpass, perfect co-location in space (400 m minimum distance) and time could be achieved. As can be seen in the four ATLID products panels (A-EBD low resolution), clear-sky conditions with aerosol up to about 3 km were observed in the entire region of interest. Because the overpass was during daytime, additional background noise occurred in both lidar measurements in contrast to the nighttime case studies discussed before. As a classical Raman lidar, the ship-borne PollyXT is not able to measure proper Raman signals at this location during daytime with the Sun almost in the zenith. Thus, only the classical Klett-Fernald approach (Klett, 1981; Fernald, 1984) could be applied. In contrast, as an HSRL, ATLID provides extinction and backscatter independently and thus also a lidar ratio profile. We used A-EBD's mean lidar ratio of Baseline BA (i.e., 65 sr for the aerosol layer from 1 to 3 km, and 20 sr for the marine boundary layer) as input for the Klett-Fernald retrieval of the ground-based system to be able to compare the two measurements quantitatively. To confirm the correct choice of lidar ratio, we also compared the integrated extinction profile of PollyXT to measurements of the AERONET Maritime Aerosol Network (MAN, Smirnov et al., 2009). The photometer measurements in the framework of MAN on RV *Meteor* (Wahl et al., 2025; MAN, 2025) led to AOD values of 0.28 at 380 nm and an Ångström exponent of 0.44. Using these values to calculate the AOD at 355 nm, we retrieve a value of 0.29. This is in perfect agreement with the ship-borne lidar observations, for which the integration of the extinction profile leads to an AOD at 355 nm of 0.30 ± 0.03. Thus, we are confident about the correct choice of the lidar ratio. The respective comparisons with Baseline AC (blue) and Baseline BA (green) are shown in Fig. 18. For Baseline BA, an excellent agreement in terms of backscatter and extinction coefficients is found between the two systems. Even though the lidar ratio of ATLID is used for the Klett retrieval of the ground-based system, the agreement in terms of magnitude and shape of the aerosol profiles between both systems is remarkable. Given the fact that the closest distance to the ground track was less than 400 m, it shows that mobile ground(ship)-based observing systems are really valuable for validation of space-borne profiles. Compared to the extinction and backscatter profiles of Baseline AC (blue lines), no major changes in Baseline BA products can be identified except for the marine boundary layer. For Baseline AC, the extinction and the lidar ratio were clearly overestimated in these

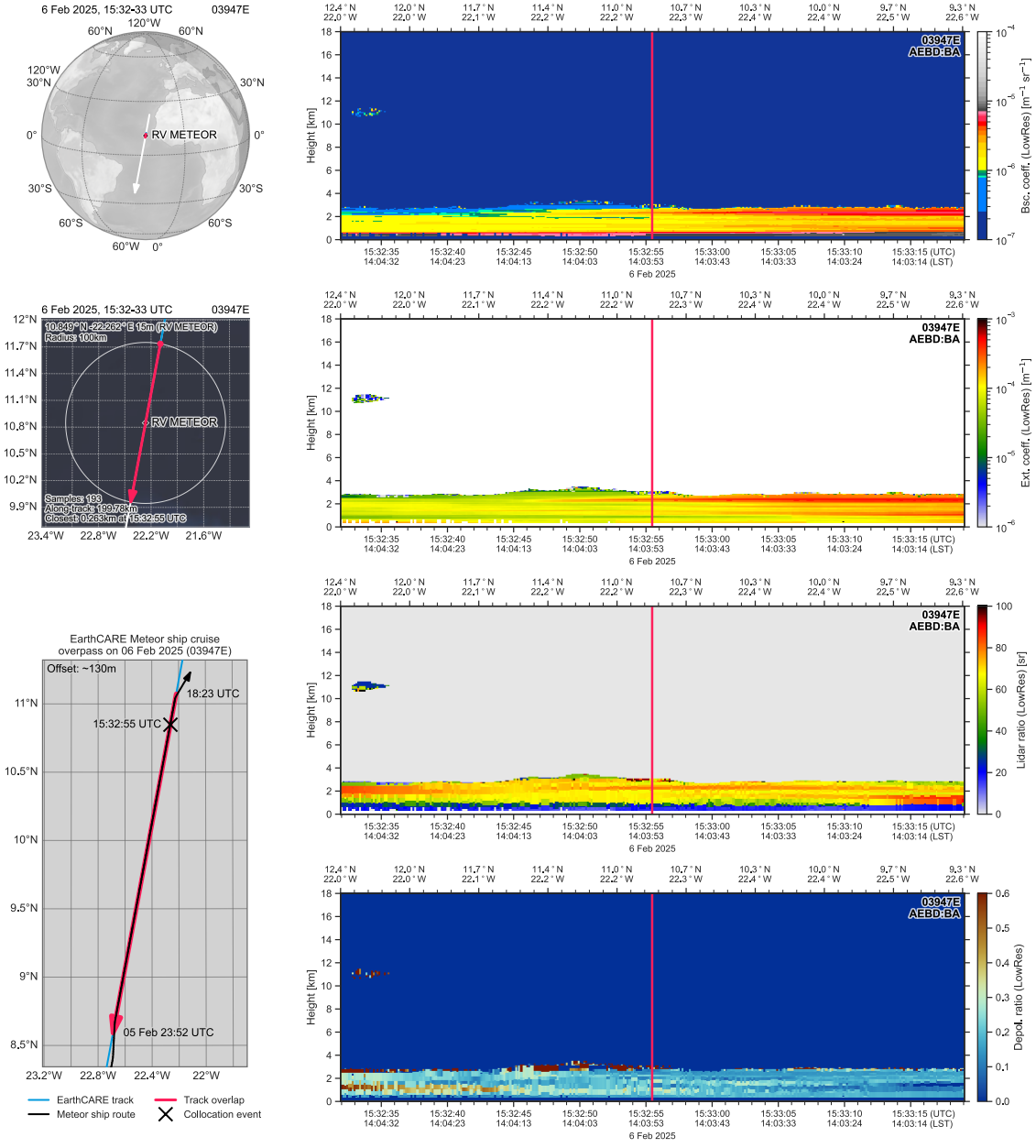

Figure 17. Same as Fig. 15, but for the overview of EarthCARE measurements on the Tropical Atlantic near 11°N, 22°W on 6 February 2025 (exact coordinates are given in the maps). The red vertical line marks the closest distance (0.26 km) to the Research Vessel *Meteor* during the overpass.

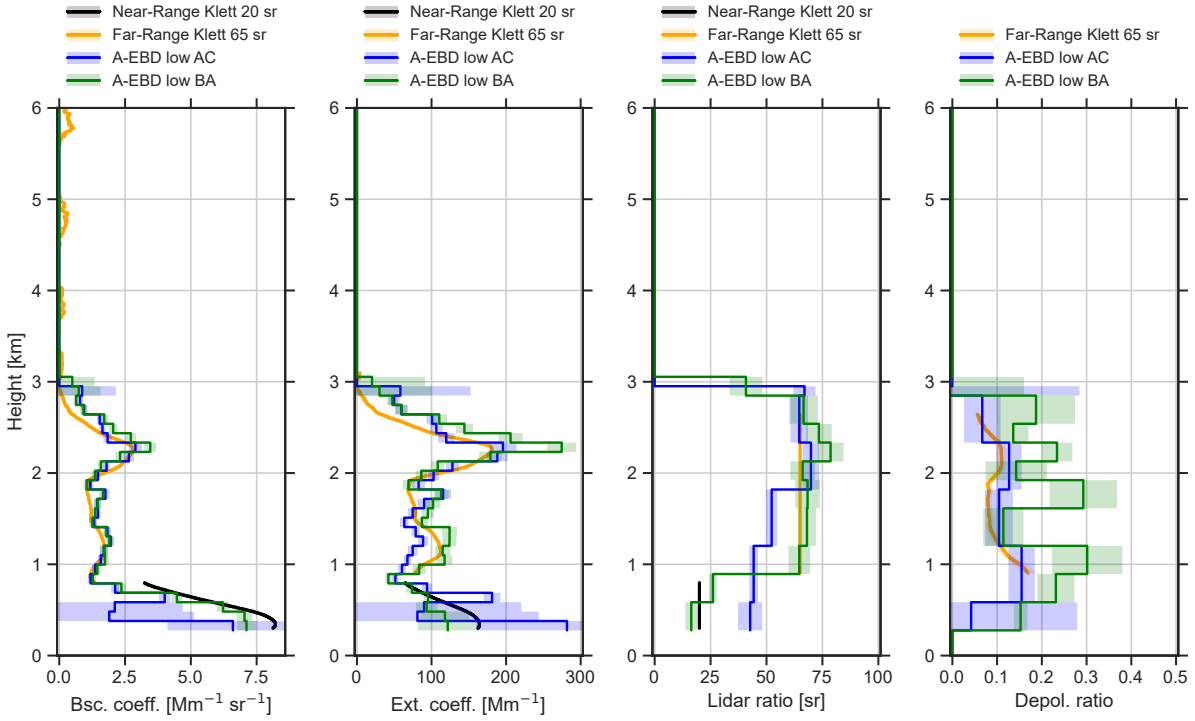

Figure 18. Comparison of EarthCARE A-EBD low-resolution products to ground-based PollyXT observations (15:22 to 15:44 UTC) on board RV *Meteor* on 6 February 2025. A-EBD products of Baseline BA (green) and Baseline AC (blue) are shown. Klett retrieval for PollyXT: Near-range profiles with lidar ratio of 20 sr, valid for marine PBL only. Far-range profiles with lidar ratio of 65 sr, valid for 1–3 km only.

marine conditions, which has significantly improved with Baseline BA. In contrast to the good agreement of backscatter and extinction, the A-EBD particle depolarization ratio values of Baseline BA (green) are generally overestimated in comparison to the ground-based reference and have obviously worsened compared to Baseline AC (blue). The PollyXT observations reveal that in the aerosol layer between 1 and 3 km, a mixture of smoke and dust from Africa was observed, leading to depolarization ratio values of 0.10. This is also in agreement with the lidar ratio observed from ATLID (lidar ratios of 70 sr indicate smoke - see, e.g., Floutsi et al., 2023). HYSPLIT and model backward trajectories confirm an air mass transport from the respective source regions (not shown). Thus, the depolarization ratio values of Baseline BA are definitely too high. Therefore, we must conclude that despite modifications in Level 1 data and in the depolarization ratio retrieval of A-EBD itself, daytime observations of moderately polarizing & scattering regimes are still prone to wrong particle depolarization ratios in Baseline BA. Further investigations are currently ongoing (e.g., Haarig et al., 2025a). We would like to stress that also for the space-borne HSRL ATLID, differences between daytime and nighttime performance occur. ATLID's cross-polarization channel is mostly affected by this increased background light due to the optical design of ATLID (Pereira do Carmo et al., 2019) with the respective consequences for the depolarization ratio product as discussed.

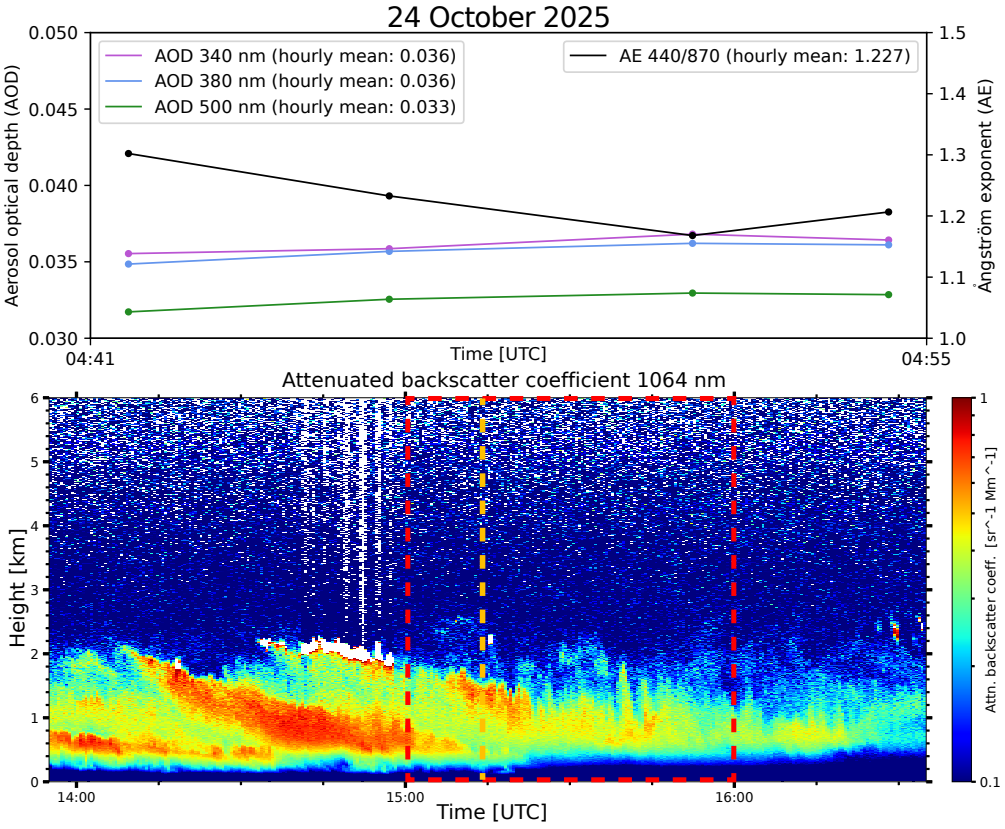

Figure 19. Top: Level 1.5 AERONET observations at Invercargill/Waihōpai, Aotearoa New Zealand, on 24 October 2025. Only observations between 04:40 and 04:55 are available. Bottom: Temporal evolution of the attenuated backscatter coefficient at 1064 nm as measured with the PollyNET lidar around the EarthCARE overpass at Invercargill/Waihōpai on 24 October 2025. EarthCARE overpass (vertical, dashed orange line) and time period for ground-based lidar analysis (dashed box) are indicated.

3.6 Pristine environment - Observations in the Southern Hemisphere

To contrast the previous case studies, which were characterized by significant aerosol load, we focus in the last case study on the pristine environment in the Southern Hemisphere, namely one observation from the goSouth-2 campaign in Southern Aotearoa New Zealand on 24 October 2025. As a side effect, we cover a completely different geographic region, which is usually undersampled with respect to ground-based profiling observations and thus of high interest for the validation of EarthCARE. During the night of interest, atmospheric conditions at the measurement site in Invercargill/Waihōpai were entirely pristine. The AOD was as low as 0.03 (last measurement of AERONET photometer on the afternoon before) as shown in Fig. 19, top. However, the atmosphere in the lowermost 2 km was quite turbulent as the time-height plot of the PollyXT attenuated backscatter coefficient at 1064 nm reveals (Fig. 19, bottom). For this reason, and because EarthCARE measurements were as close as 2.5 km to the ground-site, we do not use the A-EBD low-resolution products for comparison as before, but aim for the medium and high-

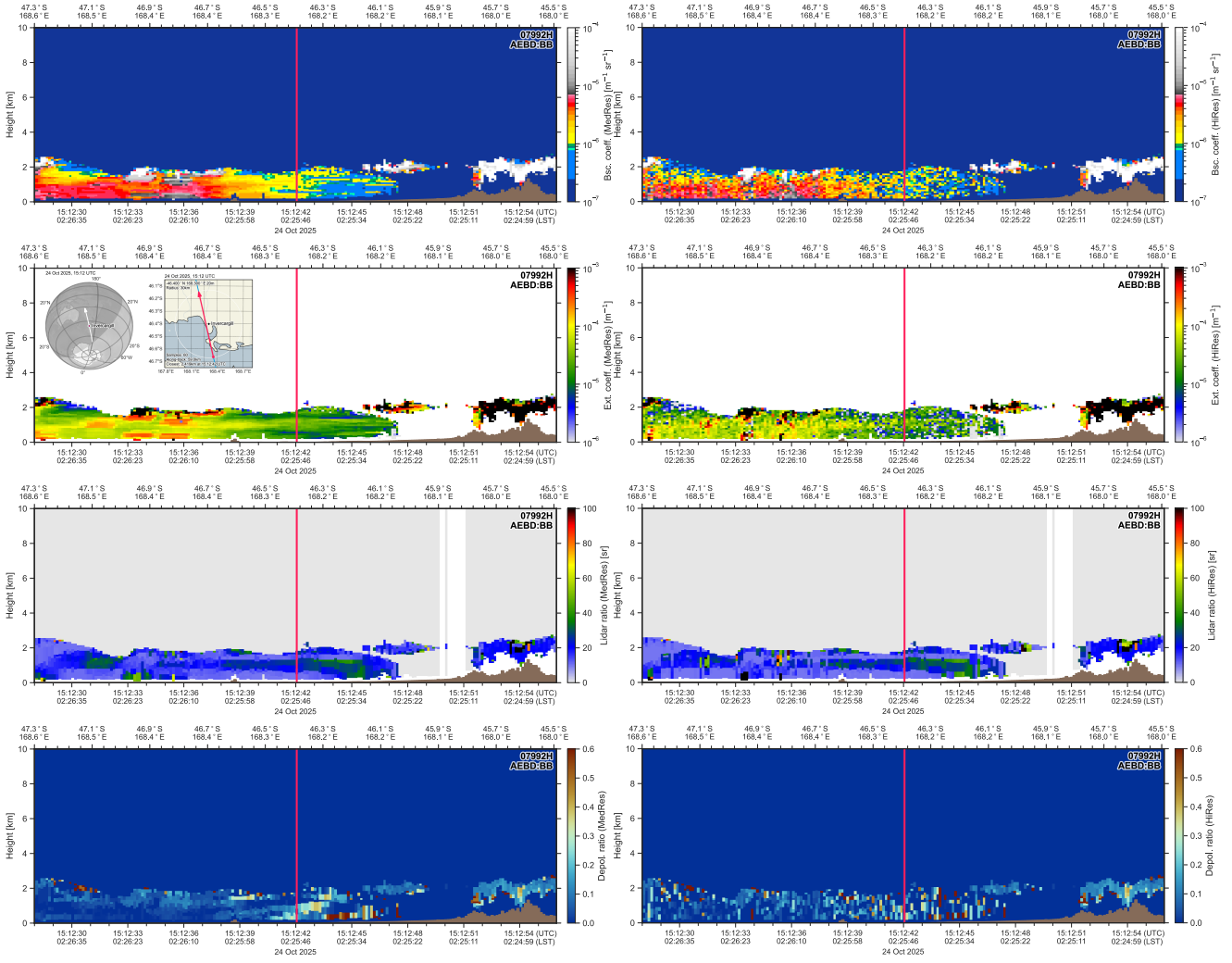

Figure 20. Overview of EarthCARE measurements on 24 October 2025 at Invercargill/Waihōpai, Aotearoa New Zealand. Time-height plots of the A-EBD product at medium (left) and high (right) resolution (Baseline BB), respectively. From top to bottom: Particle backscatter coefficient, particle extinction coefficient, particle lidar ratio and particle depolarization ratio. The red vertical line marks the closest distance (2.5 km) to the ground-based station. The maps indicating the position of the ground-track and the location of the ground-based reference site are shown this time in the second uppermost panel on the left.

resolution products. The respective geophysical quantities (backscatter and extinction coefficient, lidar and depolarization ratio) at both resolutions are shown in Fig. 20. The baseline provided is BB, the successor of BA. The medium-resolution products (left panels) show a consistent but horizontally heterogeneous structure. While the high-resolution products (right panels) seem to be dominated by noise, the general atmospheric state is still identifiable. Interestingly, the lidar ratio, which is used as *a priori* input for the optimal estimation scheme and finally provided layer-wise, shows the least scatter and is almost identical to the

medium-resolution product. The depolarization ratio product, however, is most dominated by noise (as discussed above, but here during nighttime) and obviously hardly usable in the high-resolution product for this case. Clouds around the overpass time are visible at both resolutions (remember that strong features are not smoothed in the A-EBD product) and reveal the occasional cloud formation at the top of the aerosol layer (up to 2 km), which is also visible in the PollyNET time-height cross section (see Fig. 19.) The direct comparison between the ground-based reference and the EarthCARE A-EBD products is shown in Fig. 21 for the medium and high resolutions. The low-resolution products are not shown in this Figure as well because they are not representative for near-surface atmospheric conditions due to the respective strong smoothing combined with the existing high atmospheric variability. While the high-resolution product is, of course, noisier, it shows an excellent agreement for the backscatter and extinction products, being even superior to the medium-resolution product, which shows higher values in the height region of 0.8 to 1.8 km compared to the PollyNET lidar products. Because of the strong heterogeneity of the atmospheric scene as observed by both instruments, this can be easily attributed to representativeness issues with respect to the medium-resolution products. Therefore, besides being noisy, the high-resolution products can be used and are reliable in highly dynamic regimes with low aerosol backscatter and extinction. Interestingly, the lidar ratio retrieved is as low as 10 to 13 sr for the lowermost 800 m, which is clearly a bit too low as such values have so far never been observed (see e.g., Bohlmann et al., 2018; Floutsi et al., 2023) and are also revealed by a slight underestimation of the extinction in this height range. The depolarization ratio products, however, suffer stronger from noise because of the instrument design of ATLID as discussed above (the Mie cross-polar channel is prone to more background noise, see Pereira do Carmo et al., 2019). The values of the high-resolution product agree within the uncertainties with PollyXT, but basically, the EarthCARE depolarization ratio is not usable at high resolution. For the medium resolution, it is even worse, because here the depolarization ratio strongly deviates from the ground-based reference and also shows a significant overestimation even when considering the uncertainties. The too high depolarization ratio values are most probably linked to inconsistencies in the spectral cross-talk correction. Also, the faint structures of the depolarization ratio in the clean marine BL as retrieved by EarthCARE (Fig. 20, medium resolution) might be a result of this issue, as they are not observed with the ground-based reference. Thus, it makes these ATLID depolarization ratio observations questionable.

Finally, we conclude that A-EBD backscatter and extinction products in the clean Southern Hemisphere are of excellent quality with respect to backscatter and extinction and therefore show the excellent potential of EarthCARE to study aerosol-cloud interactions in unperturbed regimes. The lidar ratios agree well except for the lowermost part of the atmosphere (below 1 km), where the values are too low and thus need some improvement.

4 Conclusions

EarthCARE, ESA's Earth Explorer Mission to investigate aerosol, clouds, radiation, and their interactions, was successfully launched in 2024. Since the beginning of the measurements with its four instruments on board, continuous improvements in instrument calibrations and retrieval algorithms have been made, resulting in several different product versions, called baselines. A first reprocessing campaign was successfully completed in September 2025, delivering for the first time a homogeneous data

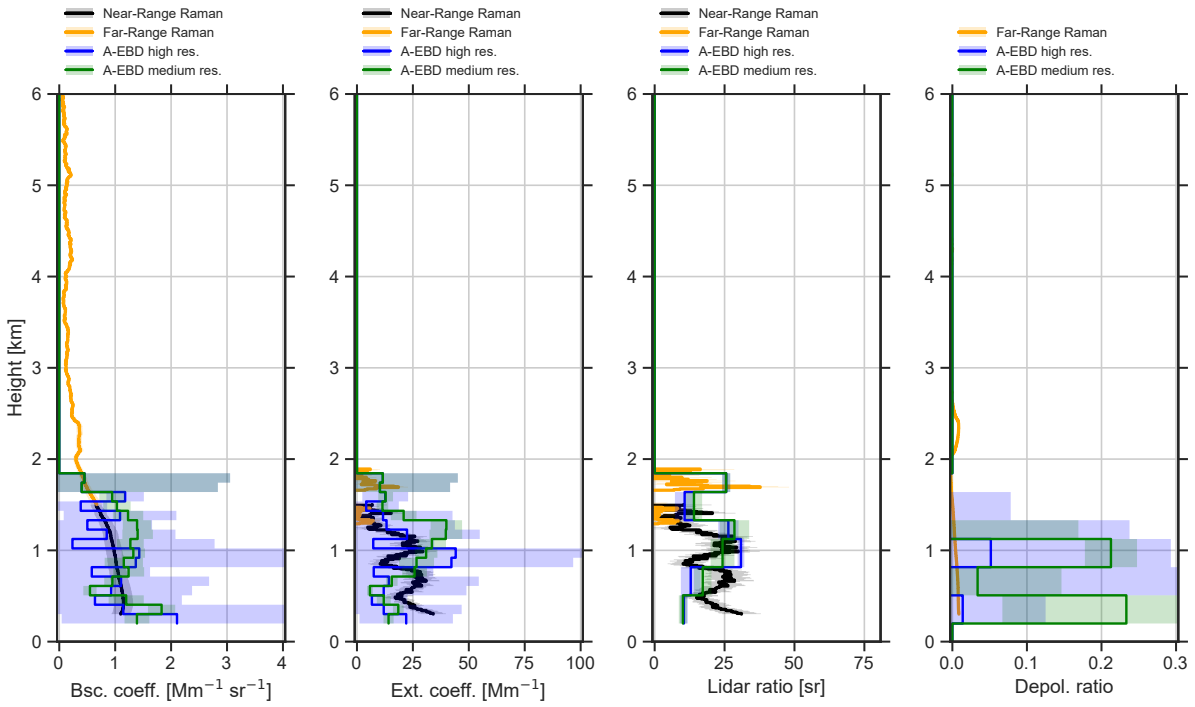

Figure 21. Comparison of EarthCARE A-EBD medium and high-resolution product (Baseline BB) to ground-based PollyXT observations at Invercargill/Waihōpai, Aotearoa New Zealand, on 24 October 2025. From left to right: Particle backscatter coefficient, particle extinction coefficient, particle lidar ratio, and particle depolarization ratio.

set processed with one baseline for the entire period from 10 August 2024 until 1 October 2025. In this work, we focused on the validation of the profiling products of EarthCARE's HSRL ATLID, namely the A-EBD and partly the A-AER product. The A-EBD product should be preferred for scientific studies as the main purpose of the A-AER product is to provide *a priori* information to A-EBD. We use the reprocessed data set retrieved with Baseline BA (BB for the last case) to give a first data quality reference for the publicly available ATLID Level 2 profiling products, which are already used for first scientific studies (e.g., Haarig et al., 2026). We analyzed and intensively discussed seven different case studies for which high-quality ground-based reference observations from PollyNET lidars were available, covering different atmospheric conditions (from dust and smoke events to ice clouds and very pristine conditions). All the case studies are characterized by a very close horizontally distance between the ATLID observations and the ground reference of less than 20 km, except for one case (75 km). With the selected case studies, several geographic locations are covered, i.e., the Tropical Atlantic, Europe, Central Asia, and the pristine Southern Hemisphere midlatitudes (Aotearoa New Zealand), providing confidence that our results are representative for ATLID in general. The findings of this paper are the following: The selected case studies reveal that EarthCARE, i.e., ATLID, has excellent profiling capabilities with remarkable signal strength and vertical resolution capabilities. We find that for all investigated atmospheric conditions (very low aerosol load to very strong scattering of ice and dust), the vertical structure

of the atmospheric features of interest could be resolved very well and match qualitatively (and mostly quantitatively) to the ground-based reference observations.

The A-EBD backscatter and extinction profiles (at low resolution) agree mostly within the provided uncertainties to the ground-based observations. Deviations from the ground-based reference were discussed and mainly found to be due to representativeness issues (e.g., to local heterogeneity in the case of the mountainous region around Dushanbe, Tajikistan) and edge effects.

The intensive particle quantity lidar ratio (extinction-to-backscatter ratio) is provided layer-wise and thus not at the same resolution as the backscatter and extinction products. It matches in many cases with the ground-based reference, but we also see some systematic deviations, e.g., a clear overestimation was observed in the case of a dust mixture near Leipzig, while an underestimation of the lidar ratio was found for very clean conditions in the Southern Hemisphere very close to the ground. This behavior is then also reflected in the extinction profiles which deviate from the ground-based reference. It is worth mentioning that A-EBD uses the lidar ratio retrieved from the A-AER processor beforehand as *a priori* input to optimize the optical profiles of ATLID (Donovan et al., 2024). Obviously, this procedure does sometimes converge to wrong values, partly because of wrong *a priori* input (coming from A-AER) together with incorrect error estimations. In the A-AER retrieval of Baseline BA, occasionally single erroneous profiles lead to erroneous lidar ratio profiles together with unrealistic error estimates. Therefore, respective lidar ratio products of Baseline BA for both A-AER and A-EBD should be used with care. The algorithm developers currently work on this issue so that such segments in the EarthCARE data can be flagged in future.

Concerning the ATLID depolarization ratio, we observe the strongest deviations from the ground-reference for this parameter and consider it in the current baselines (BA and BB) as quantitatively not reliable, except for strong scattering and depolarizing features like ice clouds (Haarig et al., 2025a). Due to ATLID's system architecture, the depolarization channel is more prone to noise, which leads to a significant day-nighttime difference in the noise levels already appearing in Level 1 data. This causes an additional offset in the daytime depolarization ratio products of EarthCARE. Sophisticated calibration and correction procedures are needed to account for this effect and correct the signals and optimize the retrievals. Many improvements have been made since the start of the measurements (Donovan, 2025), and it was demonstrated that the depolarization ratio has already significantly improved when comparing Baseline BA to AC. However, it is still not in agreement with the ground-based reference in the case of aerosol and clear-sky regimes. As the depolarization ratio is one key parameter for aerosol typing (e.g., Wandinger et al., 2023a), we identify efforts to improve this quantity as a top priority. It was found that multiple effects need to be tackled to properly correct the depolarization ratio. Currently, the EarthCARE Data Innovation & Science Cluster (DISC) is working on this topic. An updated procedure is foreseen with the release of the next major baseline (CA). Nevertheless, it is worth noting that qualitative investigations with ATLID's depolarization ratio are already possible, as the expected significant differences among different scatterer types can be identified. ATLID's depolarization ratio can thus be used to discriminate (not type) such features.

Another issue we identified are the so-called edge effects, which occur occasionally at sharp boundaries between strongly scattering and weakly scattering atmospheric features for all geophysical quantities. Obviously, the currently implemented smoothing procedure has sometimes problems handling such atmospheric conditions resulting in erroneous high values of

backscatter, extinction, and/or depolarization. Partly, these overestimates are characterized by very high error estimates and therefore can be screened out by the user. But we also found occasions when the uncertainties of the respective values were low and thus such erroneous values could only hardly be identified. In this regard, further efforts on removing or flagging such effects are needed. When comparing the products of the earlier operational Baseline AC to Baseline BA, we see an overall improvement in all ATLID products. Backscatter, extinction, and lidar ratio profiles of ATLID have mostly improved with the baseline developments, even though they already had good performance in Baseline AC. Especially, the vertical resolution of the lidar ratio products seems to be significantly improved with Baseline BA, due to the fix of an error in the assignment of sub-layers of features. Interestingly, the edge effects are less pronounced in Baseline AC compared to BA. Concluding on the findings from this paper and given the fact that EarthCARE is an ESA Earth Explorer mission deploying for the first time a UV high-spectral-resolution + depolarization lidar in space, we can state that the observing capabilities of ATLID are remarkable and have great potential to boost atmospheric science with respect to aerosol and clouds and their interaction. This became evident when, e.g., investigating the A-EBD medium (10 km horizontal resolution) and high-resolution (1 km) products for the pristine atmosphere around Aotearoa New Zealand under highly dynamic conditions. Despite the issues discussed above, an impressive quality of the medium and high-resolution extinction and backscatter products was found. This paves the way to study aerosol and clouds in very clean, unperturbed conditions, and therefore enables contrasting studies to understand the complex aerosol-cloud-radiation interaction in the Earth's atmosphere.

The main take-home message of our study is that even though EarthCARE data is public and a first reprocessing campaign has been successfully completed, the ATLID data products are not yet 100% quality assured and occasional errors in the retrieval can occur. Therefore, EarthCARE data should be intensively quality checked before using for scientific studies. It also shows that validation efforts are needed throughout the full mission lifetime, as being key for the correct interpretation of the data. The fact that the lifetime of EarthCARE has been announced to be extended from 3 to 10 (and more) years (ESA, 2025) gives a great perspective for Earth observations. There will be, of course, continuing processor developments for improved products. Validation of the new product versions will then remain key for future, but also past EarthCARE observations. As shown in this work, ground-based network observations as well as mobile facilities like the ACTRIS exploratory platforms LACROS and OCEANET are of great value for this matter, complementing the overall validation concept, including airborne, model, and satellite-to-satellite approaches.

Code availability. All plots containing EarthCARE data have been visualized using *earthcarekit* (König et al., 2025): https://pypi.org/project/earthcarekit/. TRACE was used for air mass source attribution: https://github.com/martin-rdz/trace_airmass_source.

Data availability. The EarthCARE data is available at ESA's MAAP (Multi-mission Algorithm and Analysis Platform, https://portal.maap.eo.esa.int/).

Author contributions. All authors have contributed to this work. HB conceptualized the study and drafted the manuscript together with MH. AAF, GJvZ, DD and UW contributed with expert knowledge on EarthCARE processors. EB, JH, and HG contributed with in-depth validation analysis of the used lidar data. LK developed *earthcarekit*. MR performed air mass studies, e.g., by using TRACE. BG, CJ, FF, KO, TG, AS, HBu, RE, PS, DA, AK, BH, DFN, SFA, and SKK were responsible for high-quality lidar measurements including QA procedures in the framework of ACTRIS.

Competing interests. Ulla Wandinger and Dave Donovan are members of the editorial board of AMT.

Disclaimer. The present work includes preliminary data (not fully calibrated/validated and not yet publicly released) of the EarthCARE ESA mission developed in collaboration with JAXA. The analysis has been performed in the context of the EarthCARE Validation Team (ECVT), of the ATLID Integrated Commissioning Team, and the EarthCARE Data Innovation & Science Cluster (DISC).

Acknowledgements. We sincerely acknowledge all individuals making the EarthCARE mission but also ground-based observations at several locations possible. We are also grateful for the fruitful discussions with respect to lidar profiling in the framework of EARLINET, ACTRIS, and the EarthCARE validation activities. For the Aotearoa New Zealand activities, we thank the School of Physical & Chemical Sciences of the University of Canterbury, Christchurch, and the Air Quality Collective, Auckland, for their support in setting up the measurement site at Invercargill/Waihōpai. We also appreciate the efforts of AERONET, AERONET MAN, and HYSPLIT.

The work has been primarily performed in the framework of the EarthCARE Data Innovation & Science Cluster (DISC) under ESA Contract No. 4000144997/24/I-NS and in the framework of the German Initiative for the Validation of EarthCARE (GIVE) funded by the German Federal Ministry for Economic Affairs and Energy (BMWE, grant no. 50EE2403A). Several other projects did also support our work: ACTRIS-D is funded by the German Federal Ministry of Research, Technology and Space (BMFTR, formerly the German Federal Ministry of Education and Research (BMBF), grant no. 01LK2001A) under the FONA Strategy "Research for Sustainability". Construction of a new lidar for permanent observations in Tajikistan was funded by BMBF via the PoLiCyTa project (grant no. 01LK1603A). Parts of the work have been performed in the framework of AIRSENSE (Aerosol and aerosol-cloud Interaction from Remote SENSing Enhancement) project through the contract 4000142902/23/I-NS in the framework of the ESA Atmosphere Science Cluster – Research Opportunities 5 – European Coordinated Study on Aerosols and Aerosol/Cloud Interactions. Activities in Aotearoa New Zealand are under the framework of CleanCloud - a Horizon Europe Cluster 5 project (Grant Agreement no. 101137639) project. Furthermore, the preparatory work for EarthCARE validation has been supported by the European Commission under the Horizon 2020 – Research and Innovation Framework Programme, through the ATMO-ACCESS Integrating Activity under grant agreement No 101008004.

References

Amiridis, V., Marinou, E., Hostetler, C., Koopman, R., Cecil, D., Moisseev, D., Tackett, J., Groß, S., Baars, H., Redemann, J., Marenco, F., Baldini, L., Tanelli, S., Fielding, M., Janiskova, M., Tanaka, T., O'Connor, E., Fjaeraa, A. M., Paschou, P., Voudouri, K. A., Ferrare, R., Burton, S., Schuster, G., Kato, S., Winker, D., Shook, M., Bley, S., Haarig, M., Floutsi, A. A., Wandinger, U., Trapon, D., Pfitzenmaier, L., Papagiannopoulos, N., Mona, L., Posselt, D., Mason, S., Rennie, M., Benedetti, A., Hogan, R., Sogacheva, L., Balis, D., Michailidis, K., van Zadelhoff, G.-J., Nowottnick, E., Yorks, J., Mroz, K., Donovan, D., L'Ecuyer, T., Okamoto, H., Sato, K., Henderson, D., Nishikawa, T., Barker, H., Cole, J., Qu, Z., Clerbaux, N., Nakajima, T., Chase, R., Wolff, D., Landulfo, E., Kirstetter, P.-E., Mather, J., Ohigashi, T., Ryder, C., Tzallas, V., Tsikoudi, I., Tsekeri, A., Tsichla, M., Koutsoupi, I., Kubota, T., Siomos, N., Takahashi, N., Horie, H., Suzuki, K., Mace, J., McLean, W., Borderies, M., Mangla, R., Escribano, J., Moradi, I., Zhang, J., Juli, R., Ikuta, Y., Marbach, T., Bojkov, B., Accadia, C., Fougnie, B., Spezzi, L., Bozzo, A., Chimot, J., Jafariserajehlou, S., Flament, T., Mattioli, V., Strandgren, J., Barlakas, V., and Kollias, P.: Best practice protocol for the Validation of Aerosol, Cloud, and Precipitation Profiles (ACPPV) (Version 2), https://doi.org/10.5281/zenodo.15025627, 2025.

Ansmann, A., Petzold, A., Kandler, K., Tegen, I., Wendisch, M., Müller, D., Weinzierl, B., Müller, T., and Heintzenberg, J.: Saharan Mineral Dust Experiments SAMUM-1 and SAMUM-2: what have we learned?, Tellus B, 63, 403–429, https://doi.org/10.1111/j.1600-0889.2011.00555.x, 2011.

Baars, H., Kanitz, T., Engelmann, R., Althausen, D., Heese, B., Komppula, M., Preißler, J., Tesche, M., Ansmann, A., Wandinger, U., Lim, J.-H., Ahn, J. Y., Stachlewska, I. S., Amiridis, V., Marinou, E., Seifert, P., Hofer, J., Skupin, A., Schneider, F., Bohlmann, S., Foth, A., Bley, S., Pfüller, A., Giannakaki, E., Lihavainen, H., Viisanen, Y., Hooda, R. K., Pereira, S. N., Bortoli, D., Wagner, F., Mattis, I., Janicka, L., Markowicz, K. M., Achtert, P., Artaxo, P., Pauliquevis, T., Souza, R. A. F., Sharma, V. P., van Zyl, P. G., Beukes, J. P., Sun, J., Rohwer, E. G., Deng, R., Mamouri, R.-E., and Zamorano, F.: An overview of the first decade of PollyNET: an emerging network of automated Raman-polarization lidars for continuous aerosol profiling, Atmospheric Chemistry and Physics, 16, 5111–5137, https://doi.org/10.5194/acp-16-5111-2016, 2016.

Baars, H., Seifert, P., Engelmann, R., and Wandinger, U.: Target categorization of aerosol and clouds by continuous multiwavelength-polarization lidar measurements, Atmospheric Measurement Techniques, 10, 3175–3201, https://doi.org/10.5194/amt-10-3175-2017, 2017.

Baars, H., Ansmann, A., Ohneiser, K., Haarig, M., Engelmann, R., Althausen, D., Hanssen, I., Gausa, M., Pietruczuk, A., Szkop, A., Stachlewska, I. S., Wang, D., Reichardt, J., Skupin, A., Mattis, I., Trickl, T., Vogelmann, H., Navas-Guzmán, F., Haefele, A., Acheson, K., Ruth, A. A., Tatarov, B., Müller, D., Hu, Q., Podvin, T., Goloub, P., Veselovskii, I., Pietras, C., Haeffelin, M., Fréville, P., Sicard, M., Comerón, A., Fernández García, A. J., Molero Menéndez, F., Córdoba-Jabonero, C., Guerrero-Rascado, J. L., Alados-Arboledas, L., Bortoli, D., Costa, M. J., Dionisi, D., Liberti, G. L., Wang, X., Sannino, A., Papagiannopoulos, N., Boselli, A., Mona, L., D'Amico, G., Romano, S., Perrone, M. R., Belegante, L., Nicolae, D., Grigorov, I., Gialitaki, A., Amiridis, V., Soupiona, O., Papayannis, A., Mamouri, R.-E., Nisantzi, A., Heese, B., Hofer, J., Schechner, Y. Y., Wandinger, U., and Pappalardo, G.: The unprecedented 2017–2018 stratospheric smoke event: decay phase and aerosol properties observed with the EARLINET, Atmospheric Chemistry and Physics, 19, 15 183–15 198, https://doi.org/10.5194/acp-19-15183-2019, 2019.

Baars, H., Herzog, A., Heese, B., Ohneiser, K., Hanbuch, K., Hofer, J., Yin, Z., Engelmann, R., and Wandinger, U.: Validation of Aeolus wind products above the Atlantic Ocean, Atmospheric Measurement Techniques, 13, 6007–6024, https://doi.org/10.5194/amt-13-6007-2020, 2020.

Baars, H., Radenz, M., Floutsi, A. A., Engelmann, R., Althausen, D., Heese, B., Ansmann, A., Flament, T., Dabas, A., Trapon, D., Reitebuch, O., Bley, S., and Wandinger, U.: Californian Wildfire Smoke Over Europe: A First Example of the Aerosol Observing Capabilities of Aeolus Compared to Ground-Based Lidar, Geophysical Research Letters, 48, e2020GL092 194, https://doi.org/10.1029/2020GL092194, e2020GL092194 2020GL092194, 2021.

Baars, H., Walchester, J., Basharova, E., Gebauer, H., Radenz, M., Bühl, J., Barja, B., Wandinger, U., and Seifert, P.: Long-term validation of Aeolus L2B wind products at Punta Arenas, Chile, and Leipzig, Germany, Atmospheric Measurement Techniques, 16, 3809–3834, https://doi.org/10.5194/amt-16-3809-2023, 2023.

Baars, H., Marinou, E., Mona, L., O'Connor, E., Rusli, S., Koopman, R., Fjæraa, A. M., and Nicolae, D.: The European preparation activities for the EarthCARE validation in the framework of ACTRIS/ATMO-ACCESS, in: 31st International Laser Radar Conference (ILRC-31) together with the 22nd Coherent Laser Radar Conference (CLRC), 2024.

Barker, H. W., Cole, J. N. S., Villefranque, N., Qu, Z., Velázquez Blázquez, A., Domenech, C., Mason, S. L., and Hogan, R. J.: Radiative closure assessment of retrieved cloud and aerosol properties for the EarthCARE mission: the ACMB-DF product, Atmospheric Measurement Techniques, 18, 3095–3107, https://doi.org/10.5194/amt-18-3095-2025, 2025.

Bedka, K. M., Nehrir, A. R., Kavaya, M., Barton-Grimley, R., Beaubien, M., Carroll, B., Collins, J., Cooney, J., Emmitt, G. D., Greco, S., Kooi, S., Lee, T., Liu, Z., Rodier, S., and Skofronick-Jackson, G.: Airborne lidar observations of wind, water vapor, and aerosol profiles during the NASA Aeolus calibration and validation (Cal/Val) test flight campaign, Atmospheric Measurement Techniques, 14, 4305–4334, https://doi.org/10.5194/amt-14-4305-2021, 2021.

Bley, S., Rennie, M., Žagar, N., Pinol Sole, M., Straume, A. G., Antifaev, J., Candido, S., Carver, R., Fehr, T., von Bismarck, J., Hünerbein, A., and Deneke, H.: Validation of the Aeolus L2B Rayleigh winds and ECMWF short-range forecasts in the upper troposphere and lower stratosphere using Loon super pressure balloon observations, Quarterly Journal of the Royal Meteorological Society, 148, 3852–3868, https://doi.org/10.1002/qj.4391, 2022.

Bohlmann, S., Baars, H., Radenz, M., Engelmann, R., and Macke, A.: Ship-borne aerosol profiling with lidar over the Atlantic Ocean: from pure marine conditions to complex dust–smoke mixtures, Atmospheric Chemistry and Physics, 18, 9661–9679, https://doi.org/10.5194/acp-18-9661-2018, 2018.

CARS: High Power Lidar: Standard Operation Procedures for NF operation, https://www.actris.eu/sites/default/files/inline-files/SOPs-CARS-Nov2023-v01-rev08.pdf, (last access: 20 February, 2026), 2023a.

CARS: High Power Lidar: Standard Quality Assurance Procedures for NF operation, https://www.actris.eu/sites/default/files/inline-files/QAPs-CARS-Jan2024-v01-rev12.pdf, (last access: 20 February, 2026), 2023b.

Dai, G., Wu, S., Long, W., Liu, J., Xie, Y., Sun, K., Meng, F., Song, X., Huang, Z., and Chen, W.: Aerosol and cloud data processing and optical property retrieval algorithms for the spaceborne ACDL/DQ-1, Atmospheric Measurement Techniques, 17, 1879–1890, https://doi.org/10.5194/amt-17-1879-2024, 2024.

do Carmo, J., de Villele, G., Wallace, K., Lefebvre, A., Ghose, K., Kanitz, T., Chassat, F., Corselle, B., Belhadj, T., and Bravetti, P.: ATmospheric LIDar (ATLID): Pre-Launch Testing and Calibration of the European Space Agency Instrument That Will Measure Aerosols and Thin Clouds in the Atmosphere, Atmosphere, 12, 76, 2021.

Donovan, D.: ATLID L1 Performance, in: EarthCARE Science and Validation Workshop, https://www.eorc.jaxa.jp/EARTHCARE/event/ws2025/program-data/H125_Donovan.pdf, (last access: 20 February 2026), 2025.

Donovan, D. P., van Zadelhoff, G.-J., and Wang, P.: The EarthCARE lidar cloud and aerosol profile processor (A-PRO): the A-AER, A-EBD, A-TC, and A-ICE products, Atmospheric Measurement Techniques, 17, 5301–5340, https://doi.org/10.5194/amt-17-5301-2024, 2024.

Eisinger, M., Marnas, F., Wallace, K., Kubota, T., Tomiyama, N., Ohno, Y., Tanaka, T., Tomita, E., Wehr, T., and Bernaerts, D.: The EarthCARE mission: science data processing chain overview, Atmospheric Measurement Techniques, 17, 839–862, https://doi.org/10.5194/amt-17-839-2024, 2024.

Engelmann, R., Kanitz, T., Baars, H., Heese, B., Althausen, D., Skupin, A., Wandinger, U., Komppula, M., Stachlewska, I. S., Amiridis, V., Marinou, E., Mattis, I., Linné, H., and Ansmann, A.: The automated multiwavelength Raman polarization and water-vapor lidar PollyXT: the neXT generation, Atmospheric Measurement Techniques, 9, 1767–1784, https://doi.org/10.5194/amt-9-1767-2016, 2016.

Engelmann, R., Heese, B., Skupin, A., Althausen, D., Baars, H., Jimenez, C., Gast, B., Radenz, M., and Seifert, P.: Newest 18-channel PollyNET lidar with Rotational Raman, Fluorescence, and three-wavelength-depolarization measurement capabilities, in: European Lidar Conference (ELC 2025), Hosted by University of Warsaw, 2025.

ESA: EarthCARE lifetime update: mission targets 2034 and beyond, https://earth.esa.int/eogateway/news/earthcare-lifetime-update-mission-targets-2034-and-beyond, (last access: 20 February 2026), 2025.

ESA: EarthCARE Product Data Handbook, https://earthcarehandbook.earth.esa.int/article/documentation, (last access: 20 February 2026), 2026.

Fehr, T., McCarthy, W., Amiridis, V., Baars, H., von Bismarck, J., Borne, M., Chen, S., Flamant, C., Marenco, F., Knipperz, P., Koopman, R., Lemmerz Lemmerz, C., Marinou, E., Močnik, G., Parrinello, T., Piña, A., Reitebuch, O., Skofronick-Jackson, G., Zawislak, J., and Zenk, C.: The Joint Aeolus Tropical Atlantic Campaign 2021/2022 Overview- Atmospheric Science and Satellite Validation in the Tropics, in: EGU General Assembly Conference Abstracts, EGU General Assembly Conference Abstracts, pp. EGU–7249, https://doi.org/10.5194/egusphere-egu23-7249, 2023.

Feofilov, A. G., Chepfer, H., Noël, V., Guzman, R., Gindre, C., Ma, P.-L., and Chiriaco, M.: Comparison of scattering ratio profiles retrieved from ALADIN/Aeolus and CALIOP/CALIPSO observations and preliminary estimates of cloud fraction profiles, Atmospheric Measurement Techniques, 15, 1055–1074, https://doi.org/10.5194/amt-15-1055-2022, 2022.

Fernald, F. G.: Analysis of atmospheric lidar observations: some comments, Applied Optics, 23, 652–653, https://doi.org/10.1364/AO.23.000652, 1984.

Fielding, M. D. and Janisková, M.: Direct 4D-Var assimilation of space-borne cloud radar reflectivity and lidar backscatter. Part I: Observation operator and implementation, Quarterly Journal of the Royal Meteorological Society, 146, 3877–3899, https://doi.org/10.1002/qj.3878, 2020.

Flamant, C., Chaboureau, J.-P., Delanoë, J., Gaetani, M., Jamet, C., Lavaysse, C., Bock, O., Borne, M., Cazenave, Q., Coutris, P., Cuesta, J., Menut, L., Aubry, C., Benedetti, A., Bosser, P., Bounissou, S., Caudoux, C., Collomb, H., Donal, T., Febvre, G., Fehr, T., Fink, A. H., Formenti, P., Araujo, N. G., Knippertz, P., Lecuyer, E., Andrade, M. N., Langué, C. G. N., Jonville, T., Schwarzenboeck, A., and Takeishi, A.: Cyclogenesis in the Tropical Atlantic: First Scientific Highlights from the Clouds–Atmospheric Dynamics–Dust Interactions in West Africa (CADDIWA) Field Campaign, Bulletin of the American Meteorological Society, 105, E387–E417, https://doi.org/10.1175/BAMS-D-23-0230.1, 2024.

Floutsi, A. A., Baars, H., Engelmann, R., Althausen, D., Ansmann, A., Bohlmann, S., Heese, B., Hofer, J., Kanitz, T., Haarig, M., Ohneiser, K., Radenz, M., Seifert, P., Skupin, A., Yin, Z., Abdullaev, S. F., Komppula, M., Filioglou, M., Giannakaki, E., Stachlewska, I. S., Janicka, L., Bortoli, D., Marinou, E., Amiridis, V., Gialitaki, A., Mamouri, R.-E., Barja, B., and Wandinger, U.: DeLiAn – a growing collection of depolarization ratio, lidar ratio and Ångström exponent for different aerosol types and mixtures from ground-based lidar observations, Atmospheric Measurement Techniques, 16, 2353–2379, https://doi.org/10.5194/amt-16-2353-2023, 2023.

Floutsi, A. A., Baars, H., and Wandinger, U.: HETEAC-Flex: an optimal estimation method for aerosol typing based on lidar-derived intensive optical properties, Atmospheric Measurement Techniques, 17, 693–714, https://doi.org/10.5194/amt-17-693-2024, 2024.

Floutsi, A. A., Rizos, K., Trapon, D., Engelmann, R., Althausen, D., Marinou, E., Paschou, P., Hofer, J., Proestakis, E., Gebauer, H., Skupin, A., Ansmann, A., Fehr, T., Hummel, T., Koopman, R., Amiridis, V., Wandinger, U., and Baars, H.: On the representativeness of the ground-based lidar observations for satellite calibration/validation – the example of the archipelago of Cabo Verde, Atmospheric Measurement Techniques, 19, 1901–1925, https://doi.org/10.5194/amt-19-1901-2026, 2026.

Freudenthaler, V.: The telecover test: A quality assurance tool for the optical part of a lidar system, in: 24^{th} International Laser Radar Conference, Boulder, CO, presentation: S01P-3, 2008.

Freudenthaler, V.: About the effects of polarising optics on lidar signals and the Δ90 calibration, Atmospheric Measurement Techniques, 9, 4181–4255, https://doi.org/10.5194/amt-9-4181-2016, 2016.

Freudenthaler, V., Esselborn, M., Wiegner, M., Heese, B., Tesche, M., Ansmann, A., Müller, D., Althausen, D., Wirth, M., Fix, A., Ehret, G., Knippertz, P., Toledano, C., Gasteiger, J., Garhammer, M., and Seefeldner, M.: Depolarization ratio profiling at several wavelengths in pure Saharan dust during SAMUM 2006, Tellus B, 61, 165–179, https://doi.org/10.1111/j.1600-0889.2008.00396.x, 2009.

Gast, B., Jimenez, C., Ansmann, A., Haarig, M., Engelmann, R., Fritzsch, F., Floutsi, A. A., Griesche, H., Ohneiser, K., Hofer, J., Radenz, M., Baars, H., Seifert, P., and Wandinger, U.: Invisible aerosol layers: improved lidar detection capabilities by means of laser-induced aerosol fluorescence, Atmospheric Chemistry and Physics, 25, 3995–4011, https://doi.org/10.5194/acp-25-3995-2025, 2025.

Gast, B., Jimenez, C., Ansmann, A., Baars, H., and Wandinger, U.: Lidar ratios and fluorescence properties of stratospheric volcanic sulfate, ESS Open Archive, 2026, https://doi.org/10.22541/essoar.15002924/v1, 2026.

Gebauer, H., Floutsi, A. A., Haarig, M., Radenz, M., Engelmann, R., Althausen, D., Skupin, A., Ansmann, A., Zenk, C., and Baars, H.: Tropospheric sulfate from Cumbre Vieja (La Palma) observed over Cabo Verde contrasted with background conditions: a lidar case study of aerosol extinction, backscatter, depolarization and lidar ratio profiles at 355, 532 and 1064 nm, Atmospheric Chemistry and Physics, 24, 5047–5067, https://doi.org/10.5194/acp-24-5047-2024, 2024.

Gebauer, H., König, L., Baars, H., Floutsi, A. A., Haarig, M., Engelmann, R., Skupin, A., Fritzsch, F., Gaudek, T., Gast, B., Neves, L., and Wandinger, U.: Validation of EarthCARE L2a products using ground-based lidar measurements at Cabo Verde, Tajikistan and Germany in the framework of the German Initiative for the Validation, in: 2nd EarthCARE Cal/Val Workshop, 2025.

Gebauer, H., Floutsi, A. A., Hofer, J., Haarig, M., Skupin, A., Engelmann, R., Jimenez, C., Wagner, R., and Baars, H.: Characterization of the annual cycle of atmospheric aerosol over Mindelo, Cabo Verde, by means of continuous multiwavelength lidar observations, Atmospheric Chemistry and Physics, 26, 3439–3465, https://doi.org/10.5194/acp-26-3439-2026, 2026.

GEOMAR: Long-term measurements for climate research - “WARD Tropics” Expedition studies ocean currents in the tropical Atlantic, https://www.geomar.de/en/news/article/langzeitmessungen-fuer-die-klimaforschung, (last access: 20 February, 2026), 2025a.

GEOMAR: METEOR (III) [1986-2026] M207, https://www.geomar.de/en/research/expeditions/detail-view/exp/370971?cHash=42b9d051160bb67263cd14349afdf4de, (last access: 20 February, 2026), 2025b.

Gkikas, A., Gialitaki, A., Binietoglou, I., Marinou, E., Tsichla, M., Siomos, N., Paschou, P., Kampouri, A., Voudouri, K. A., Proestakis, E., Mylonaki, M., Papanikolaou, C.-A., Michailidis, K., Baars, H., Straume, A. G., Balis, D., Papayannis, A., Parrinello, T., and Amiridis, V.: First assessment of Aeolus Standard Correct Algorithm particle backscatter coefficient retrievals in the eastern Mediterranean, Atmospheric Measurement Techniques, 16, 1017–1042, https://doi.org/10.5194/amt-16-1017-2023, 2023.

Groß, S., Tesche, M., Freudenthaler, V., Toledano, C., Wiegner, M., Ansmann, A., Althausen, D., and Seefeldner, M.: Characterization of Saharan dust, marine aerosols and mixtures of biomass-burning aerosols and dust by means of multi-wavelength depolarization and Raman lidar measurements during SAMUM 2, Tellus B, 63, 706–724, https://doi.org/10.1111/j.1600-0889.2011.00556.x, 2011.

Groß, S., Ewald, F., Stevens, B., Wirth, M., Dekoutsidis, G., Ehrlich, A., Kouklaki, D., Krüger, K., Rosenburg, S., Volkmer, L., von Bismark, J., Hirsch, L., Luebke, A. E., Marinou, E., Mayer, B., Pinol Sole, M., Wendisch, M., Windmiller, J., Amiridis, V., Koopman, R., Kubota, T., and Rapp, M.: Persistent EarthCARE underflight studies of the ITCZ and organized convection (PERCUSION): Contribution to EarthCARE Validation, EGUsphere, 2026, 1–41, https://doi.org/10.5194/egusphere-2026-112, 2026.

Haarig, M., Ansmann, A., Gasteiger, J., Kandler, K., Althausen, D., Baars, H., Radenz, M., and Farrell, D. A.: Dry versus wet marine particle optical properties: RH dependence of depolarization ratio, backscatter, and extinction from multiwavelength lidar measurements during SALTRACE, Atmospheric Chemistry and Physics, 17, 14 199–14 217, https://doi.org/10.5194/acp-17-14199-2017, 2017.

Haarig, M., Ansmann, A., Baars, H., Jimenez, C., Veselovskii, I., Engelmann, R., and Althausen, D.: Depolarization and lidar ratios at 355, 532, and 1064 nm and microphysical properties of aged tropospheric and stratospheric Canadian wildfire smoke, Atmospheric Chemistry and Physics, 18, 11 847–11 861, https://doi.org/10.5194/acp-18-11847-2018, 2018.

Haarig, M., Ansmann, A., Engelmann, R., Baars, H., Toledano, C., Torres, B., Althausen, D., Radenz, M., and Wandinger, U.: First triple-wavelength lidar observations of depolarization and extinction-to-backscatter ratios of Saharan dust, Atmospheric Chemistry and Physics, 22, 355–369, https://doi.org/10.5194/acp-22-355-2022, 2022.

Haarig, M., Hünerbein, A., Wandinger, U., Docter, N., Bley, S., Donovan, D., and van Zadelhoff, G.-J.: Cloud top heights and aerosol columnar properties from combined EarthCARE lidar and imager observations: the AM-CTH and AM-ACD products, Atmospheric Measurement Techniques, 16, 5953–5975, https://doi.org/10.5194/amt-16-5953-2023, 2023.

Haarig, M., Donovan, D., Chantry, A., Marnas, F., König, L., Baars, H., Jin, Y., Nishizawa, T., Tsichla, M., Voudouri, K. A., Marinou, E., Panahifar, H., Poutli, M., Mamouri, R., Gouveia, D., Apituley, A., Wang, P., Hair, J., Shingler, T., Ferrare, R., Hostetler, C., Groß, S., Wirth, M., Engelmann, R., Gebauer, H., Floutsi, A. A., Hofer, J., van Zadelhoff, G.-J., and Wandinger, U.: Validation of ATLID's L1 and L2 depolarization ratio products, in: EarthCARE Science and Validation Workshop, https://www.eorc.jaxa.jp/EARTHCARE/event/ws2025/program-data/H408_Haarig_ATLID_Depolvalidation.pdf, (last access: 20 February, 2026), 2025a.

Haarig, M., Donovan, D., Wandinger, U., Marnas, F., Chantry, A., König, L., van Zadelhoff, G.-J., Gebauer, H., Hofer, J., Floutsi, A., and Baars, H.: The validation of the depolarization ratio measured by ATLID, in: ESA Living Planet Symposium, 2025b.

Haarig, M., Baars, H., König, L., Donovan, D. P., Ansmann, A., Khaykin, S., Ceolato, R., Gast, B., Jimenez, C., Floutsi, A. A., Hogan, R. J., Chantry, A., Marnas, F., Roschke, J., Zadelhoff, G.-J. v., and Wandinger, U.: The Life Cycle of a Stratospheric Smoke Plume as Seen From EarthCARE—Tracking a Plume From Canada to Europe, Geophysical Research Letters, 53, e2025GL119 977, https://doi.org/https://doi.org/10.1029/2025GL119977, e2025GL119977 2025GL119977, 2026.

Heese, B., Engelmann, R., Baars, H., Kompula, M., Klamt, A., and Althausen, D.: PollyNET – A lidar Network, in: European Lidar Conference (ELC 2025), Hosted by University of Warsaw, 2025.

Hofer, J., Althausen, D., Abdullaev, S. F., Makhmudov, A. N., Nazarov, B. I., Schettler, G., Engelmann, R., Baars, H., Fomba, K. W., Müller, K., Heinold, B., Kandler, K., and Ansmann, A.: Long-term profiling of mineral dust and pollution aerosol with multiwavelength polarization Raman lidar at the Central Asian site of Dushanbe, Tajikistan: case studies, Atmospheric Chemistry and Physics, 17, 14 559–14 577, https://doi.org/10.5194/acp-17-14559-2017, 2017.

Hofer, J., Ansmann, A., Althausen, D., Engelmann, R., Baars, H., Abdullaev, S. F., and Makhmudov, A. N.: Long-term profiling of aerosol light extinction, particle mass, cloud condensation nuclei, and ice-nucleating particle concentration over Dushanbe, Tajikistan, in Central Asia, Atmospheric Chemistry and Physics, 20, 4695–4711, https://doi.org/10.5194/acp-20-4695-2020, 2020a.

Hofer, J., Ansmann, A., Althausen, D., Engelmann, R., Baars, H., Fomba, K. W., Wandinger, U., Abdullaev, S. F., and Makhmudov, A. N.: Optical properties of Central Asian aerosol relevant for spaceborne lidar applications and aerosol typing at 355 and 532 nm, Atmospheric Chemistry and Physics, 20, 9265–9280, https://doi.org/10.5194/acp-20-9265-2020, 2020b.

Hummels, R.: Master tracks in different resolutions of METEOR cruise M207, Belem - Mindelo, 2025-01-04 - 2025-02-11, https://doi.org/10.1594/PANGAEA.981480, 2025.

Irbah, A., Delanoë, J., van Zadelhoff, G.-J., Donovan, D. P., Kollias, P., Puigdomènech Treserras, B., Mason, S., Hogan, R. J., and Tatarevic, A.: The classification of atmospheric hydrometeors and aerosols from the EarthCARE radar and lidar: the A-TC, C-TC and AC-TC products, Atmospheric Measurement Techniques, 16, 2795–2820, https://doi.org/10.5194/amt-16-2795-2023, 2023.

Janisková, M. and Fielding, M. D.: Direct 4D-Var assimilation of space-borne cloud radar and lidar observations. Part II: Impact on analysis and subsequent forecast, Quarterly Journal of the Royal Meteorological Society, 146, 3900–3916, https://doi.org/10.1002/qj.3879, 2020.

Kanitz, T., Ansmann, A., Foth, A., Seifert, P., Wandinger, U., Engelmann, R., Baars, H., Althausen, D., Casiccia, C., and Zamorano, F.: Surface matters: limitations of CALIPSO V3 aerosol typing in coastal regions, Atmospheric Measurement Techniques, 7, 2061–2072, https://doi.org/10.5194/amt-7-2061-2014, 2014.

Khaykin, S., Sicard, M., Leblanc, T., Sakai, T., Balugin, N., Berthet, G., Chevrier, S., Chouza, F., Feofilov, A., Gantois, D., Godin-Beekmann, S., Haddouche, A., Jin, Y., Morino, I., Kadygrov, N., Lecas, T., Liley, B., Querel, R., Taha, G., and Yushkov, V.: Global transport of stratospheric aerosol produced by Ruang eruption from EarthCARE ATLID, limb-viewing satellites and ground-based lidar observations, Atmospheric Chemistry and Physics, 26, 607–622, https://doi.org/10.5194/acp-26-607-2026, 2026.

Kim, M.-H., Kim, S.-W., Yoon, S.-C., and Omar, A. H.: Comparison of aerosol optical depth between CALIOP and MODIS-Aqua for CALIOP aerosol subtypes over the ocean, Journal of Geophysical Research: Atmospheres, 118, 13,241–13,252, https://doi.org/10.1002/2013JD019527, 2013.

Klamt, A., Yin, Z., Floutsi, A. A., Griesche, H., Haarig, M., Radenz, M., Jimenez, C., Gast, B., and Baars, H.: PollyNET: Pollynet Processing Chain, https://doi.org/10.5281/zenodo.13379737, 2024.

Klett, J. D.: Stable analytical inversion solution for processing lidar returns, Applied Optics, 20, 211–220, https://doi.org/10.1364/AO.20.000211, 1981.

Kubota, T., Kikuchi, M., Muto, M., Hashimoto, M., Imura, Y., Maruyama, K., Hoffmann, A., Hummel, T., Koopman, R., Malina, E., Rusli, S., Tzallas, V., von Bismarck, J., and Frommknecht, B.: Summary of the EarthCARE science and validation workshop 2025 -Early achievements and future perspectives for the Earth Cloud Aerosol and Radiation Explorer (EarthCARE) satellite mission-, Journal of the European Meteorological Society, 4, 100 037, https://doi.org/https://doi.org/10.1016/j.jemets.2026.100037, 2026.

König, L., Floutsi, A. A., Haarig, M., Baars, H., Mason, S., and Wandinger, U.: earthcarekit: A Python package to simplify working with EarthCARE satellite data, https://doi.org/10.5281/zenodo.16813294, 2025.

Laj, P., Myhre, C. L., Riffault, V., Amiridis, V., Fuchs, H., Eleftheriadis, K., Petäjä, T., Salameh, T., Kivekäs, N., Juurola, E., Saponaro, G., Philippin, S., Cornacchia, C., Arboledas, L. A., Baars, H., Claude, A., Mazière, M. D., Dils, B., Dufresne, M., Evangeliou, N., Favez, O., Fiebig, M., Haeffelin, M., Herrmann, H., Höhler, K., Illmann, N., Kreuter, A., Ludewig, E., Marinou, E., Möhler, O., Mona, L., Murberg, L. E., Nicolae, D., Novelli, A., O'Connor, E., Ohneiser, K., Altieri, R. M. P., Picquet-Varrault, B., van Pinxteren, D., Pospichal, B., Putaud, J.-P., Reimann, S., Siomos, N., Stachlewska, I., Tillmann, R., Voudouri, K. A., Wandinger, U., Wiedensohler, A., Apituley, A., Comerón,

A., Gysel-Beer, M., Mihalopoulos, N., Nikolova, N., Pietruczuk, A., Sauvage, S., Sciare, J., Skov, H., Svendby, T., Swietlicki, E., Tonev, D., Vaughan, G., Zdimal, V., Baltensperger, U., Doussin, J.-F., Kulmala, M., Pappalardo, G., Sundet, S. S., and Vana, M.: Aerosol, Clouds and Trace Gases Research Infrastructure – ACTRIS, the European research infrastructure supporting atmospheric science, Bulletin of the American Meteorological Society, https://doi.org/10.1175/BAMS-D-23-0064.1, 2024.

Liu, Q., Huang, Z., Liu, J., Chen, W., Dong, Q., Wu, S., Dai, G., Li, M., Li, W., Li, Z., Song, X., and Xie, Y.: Validation of initial observation from the first spaceborne high-spectral-resolution lidar with a ground-based lidar network, Atmospheric Measurement Techniques, 17, 1403–1417, https://doi.org/10.5194/amt-17-1403-2024, 2024.

Lux, O., Lemmerz, C., Weiler, F., Marksteiner, U., Witschas, B., Rahm, S., Geiß, A., and Reitebuch, O.: Intercomparison of wind observations from the European Space Agency's Aeolus satellite mission and the ALADIN Airborne Demonstrator, Atmospheric Measurement Techniques, 13, 2075–2097, https://doi.org/10.5194/amt-13-2075-2020, 2020.

Mamouri, R. E., Amiridis, V., Papayannis, A., Giannakaki, E., Tsaknakis, G., and Balis, D. S.: Validation of CALIPSO space-borne-derived attenuated backscatter coefficient profiles using a ground-based lidar in Athens, Greece, Atmospheric Measurement Techniques, 2, 513–522, https://doi.org/10.5194/amt-2-513-2009, 2009.

MAN: 2025 RV Meteor Cruise, https://aeronet.gsfc.nasa.gov/new_web/cruises_v3/Meteor_25_0.html, (last access: 24 April 2026), 2025.

Marinou, E., Paschou, P., Tsikoudi, I., Tsekeri, A., Daskalopoulou, V., Kouklaki, D., Siomos, N., Spanakis-Misirlis, V., Voudouri, K. A., Georgiou, T., Drakaki, E., Kampouri, A., Papachristopoulou, K., Mavropoulou, I., Mallios, S., Proestakis, E., Gkikas, A., Koutsoupi, I., Raptis, I. P., Kazadzis, S., Baars, H., Floutsi, A., Pirloaga, R., Nemuc, A., Marenco, F., Kezoudi, M., Papetta, A., Močnik, G., Díez, J. Y., Ryder, C. L., Ratcliffe, N., Kandler, K., Sudharaj, A., and Amiridis, V.: An Overview of the ASKOS Campaign in Cabo Verde, Environmental Sciences Proceedings, 26, https://doi.org/10.3390/environsciproc2023026200, 2023.

Marinou, E., Baars, H., Mona, L., O'Connor, E., Rusli, S., Koopman, R., Fjæraa, A. M., and Nicolae, D.: Actris, Earlinet, and Cloudnet Cal/Val Contribution to Earthcare Mission, IEEE Xplore, IGARSS 2024 - 2024 IEEE International Geoscience and Remote Sensing Symposium, Athens, Greece, 07-12 July 2024, pp. 3108–3110, https://doi.org/10.1109/IGARSS53475.2024.10642457, 2024.

Marseille, G.-J., de Kloe, J., Marksteiner, U., Reitebuch, O., Rennie, M., and de Haan, S.: NWP calibration applied to Aeolus Mie channel winds, Quarterly Journal of the Royal Meteorological Society, 148, 1020–1034, https://doi.org/10.1002/qj.4244, 2022.

Mason, S. L., Hogan, R. J., Bozzo, A., and Pounder, N. L.: A unified synergistic retrieval of clouds, aerosols, and precipitation from EarthCARE: the ACM-CAP product, Atmospheric Measurement Techniques, 16, 3459–3486, https://doi.org/10.5194/amt-16-3459-2023, 2023.

Mattis, I., Ansmann, A., Müller, D., Wandinger, U., and Althausen, D.: Multiyear aerosol observations with dual-wavelength Raman lidar in the framework of EARLINET, Journal of Geophysical Research: Atmospheres, 109, https://doi.org/10.1029/2004JD004600, 2004.

Müller, G. H., Floutsi, A. A., Baars, H., Hofer, J., Engelmann, R., Althausen, D., Abdullaev, S. F., and Khalifaeva, S.: Annual aerosol and dust cycle observed by lidar in Central Asia, Dushanbe, Tajikistan, in: European Lidar Conference (ELC 2025), 2025.

Nishizawa, T., Kudo, R., Oikawa, E., Higurashi, A., Jin, Y., Sugimoto, N., Sato, K., and Okamoto, H.: Algorithms to retrieve aerosol optical properties using lidar measurements on board the EarthCARE satellite, Atmospheric Measurement Techniques, 19, 729–744, https://doi.org/10.5194/amt-19-729-2026, 2026.

Omar, A. H., Winker, D. M., Tackett, J. L., Giles, D. M., Kar, J., Liu, Z., Vaughan, M. A., Powell, K. A., and Trepte, C. R.: CALIOP and AERONET aerosol optical depth comparisons: One size fits none, Journal of Geophysical Research: Atmospheres, 118, 4748–4766, https://doi.org/10.1002/jgrd.50330, 2013.

Papagiannopoulos, N., Mona, L., Alados-Arboledas, L., Amiridis, V., Baars, H., Binietoglou, I., Bortoli, D., D'Amico, G., Giunta, A., Guerrero-Rascado, J. L., Schwarz, A., Pereira, S., Spinelli, N., Wandinger, U., Wang, X., and Pappalardo, G.: CALIPSO climatological

products: Evaluation and suggestions from EARLINET, Atmospheric Chemistry and Physics, 16, 2341–2357, https://doi.org/10.5194/acp-16-2341-2016, 2016.

Pappalardo, G., Wandinger, U., Mona, L., Hiebsch, A., Mattis, I., Amodeo, A., Ansmann, A., Seifert, P., Linné, H., Apituley, A., Alados Arboledas, L., Balis, D., Chaikovsky, A., D´Amico, G., De Tomasi, F., Freudenthaler, V., Giannakaki, E., Giunta, A., Grigorov, I., Iarlori, M., Madonna, F., Mamouri, R.-E., Nasti, L., Papayannis, A., Pietruczuk, A., Pujadas, M., Rizi, V., Rocadenbosch, F., Russo, F., Schnell, F., Spinelli, N., Wang, X., and Wiegner, M.: EARLINET correlative measurements for CALIPSO: First intercomparison results, Journal of Geophysical Research - Atmospheres, 115, https://doi.org/10.1029/2009JD012147, 2010.

Pappalardo, G., Amodeo, A., Apituley, A., Comeron, A., Freudenthaler, V., Linné, H., Ansmann, A., Bösenberg, J., D'Amico, G., Mattis, I., Mona, L., Wandinger, U., Amiridis, V., Alados-Arboledas, L., Nicolae, D., and Wiegner, M.: EARLINET: towards an advanced sustainable European aerosol lidar network, Atmospheric Measurement Techniques, 7, 2389–2409, https://doi.org/10.5194/amt-7-2389-2014, 2014.

Paschou, P., Siomos, N., Marinou, E., Gkikas, A., Idrissa, S. M., Quaye, D. T., Fiogbe Attannon, D. D., Voudouri, K. A., Meleti, C., Donovan, D. P., Georgoussis, G., Parrinello, T., Fehr, T., von Bismarck, J., and Amiridis, V.: Validation of the Aeolus L2A products with the eVe reference lidar measurements from the ASKOS/JATAC campaign, Atmospheric Measurement Techniques, 18, 4731–4754, https://doi.org/10.5194/amt-18-4731-2025, 2025.

Pauly, R. M., Yorks, J. E., Hlavka, D. L., McGill, M. J., Amiridis, V., Palm, S. P., Rodier, S. D., Vaughan, M. A., Selmer, P. A., Kupchock, A. W., Baars, H., and Gialitaki, A.: Cloud Aerosol Transport System (CATS) 1064 nm calibration and validation, Atmospheric Measurement Techniques, 12, 6241–6258, https://doi.org/10.5194/amt-12-6241-2019, 2019.

Pereira do Carmo, J., de Villele, G., Helière, A., Wallace, K., Lefebvre, A., and Chassat, F.: ATLID, ESA atmospheric backscatter LIDAR for the ESA EarthCARE mission, CEAS Space Journal, 11, 423–435, https://doi.org/10.3390/atmos12010076, 2019.

Peuch, V.-H., Engelen, R., Rixen, M., Dee, D., Flemming, J., Suttie, M., Ades, M., Agustí-Panareda, A., Ananasso, C., Andersson, E., Armstrong, D., Barré, J., Bousserez, N., Dominguez, J. J., Garrigues, S., Inness, A., Jones, L., Kipling, Z., Letertre-Danczak, J., Parrington, M., Razinger, M., Ribas, R., Vermoote, S., Yang, X., Simmons, A., de Marcilla, J. G., and Thépaut, J.-N.: The Copernicus Atmosphere Monitoring Service: From Research to Operations, Bulletin of the American Meteorological Society, 103, E2650–E2668, https://doi.org/10.1175/BAMS-D-21-0314.1, 2022.

Proestakis, E., Amiridis, V., Marinou, E., Binietoglou, I., Ansmann, A., Wandinger, U., Hofer, J., Yorks, J., Nowottnick, E., Makhmudov, A., Papayannis, A., Pietruczuk, A., Gialitaki, A., Apituley, A., Szkop, A., Muñoz Porcar, C., Bortoli, D., Dionisi, D., Althausen, D., Mamali, D., Balis, D., Nicolae, D., Tetoni, E., Liberti, G. L., Baars, H., Mattis, I., Stachlewska, I. S., Voudouri, K. A., Mona, L., Mylonaki, M., Perrone, M. R., Costa, M. J., Sicard, M., Papagiannopoulos, N., Siomos, N., Burlizzi, P., Pauly, R., Engelmann, R., Abdullaev, S., and Pappalardo, G.: EARLINET evaluation of the CATS Level 2 aerosol backscatter coefficient product, Atmospheric Chemistry and Physics, 19, 11 743–11 764, https://doi.org/10.5194/acp-19-11743-2019, 2019.

Radenz, M., Bühl, J., Seifert, P., Baars, H., Engelmann, R., Barja González, B., Mamouri, R.-E., Zamorano, F., and Ansmann, A.: Hemispheric contrasts in ice formation in stratiform mixed-phase clouds: disentangling the role of aerosol and dynamics with ground-based remote sensing, Atmospheric Chemistry and Physics, 21, 17 969–17 994, https://doi.org/10.5194/acp-21-17969-2021, 2021a.

Radenz, M., Seifert, P., Baars, H., Floutsi, A. A., Yin, Z., and Bühl, J.: Automated time–height-resolved air mass source attribution for profiling remote sensing applications, Atmospheric Chemistry and Physics, 21, 3015–3033, https://doi.org/10.5194/acp-21-3015-2021, 2021b.

Radenz, M., Engelmann, R., Henning, S., Schmithüsen, H., Baars, H., Frey, M. M., Weller, R., Bühl, J., Jimenez, C., Roschke, J., Muser, L. O., Wullenweber, N., Zeppenfeld, S., Griesche, H., Wandinger, U., and Seifert, P.: Ground-Based Remote Sensing of Aerosol, Clouds,

Dynamics, and Precipitation in Antarctica: First Results from the 1-Year COALA Campaign at Neumayer Station III in 2023, Bulletin of the American Meteorological Society, 105, E1438–E1457, https://doi.org/10.1175/BAMS-D-22-0285.1, 2024.

Redemann, J., Vaughan, M. A., Zhang, Q., Shinozuka, Y., Russell, P. B., Livingston, J. M., Kacenelenbogen, M., and Remer, L. A.: The comparison of MODIS-Aqua (C5) and CALIOP (V2 & V3) aerosol optical depth, Atmospheric Chemistry and Physics, 12, 3025–3043, https://doi.org/10.5194/acp-12-3025-2012, 2012.

Reitebuch, O.: Challenges and achievements of ESA´s Aeolus mission, in: International Conference on Space Optics — ICSO 2024, edited by Bernard, F., Karafolas, N., Kubik, P., and Minoglou, K., vol. 13699, p. 136990T, International Society for Optics and Photonics, SPIE, https://doi.org/10.1117/12.3072760, 2025.

Rittmeister, F., Ansmann, A., Engelmann, R., Skupin, A., Baars, H., Kanitz, T., and Kinne, S.: Profiling of Saharan dust from the Caribbean to western Africa – Part 1: Layering structures and optical properties from shipborne polarization/Raman lidar observations, Atmospheric Chemistry and Physics, 17, 12 963–12 983, https://doi.org/10.5194/acp-17-12963-2017, 2017.

Rogers, R. R., Hostetler, C. A., Hair, J. W., Ferrare, R. A., Liu, Z., Obland, M. D., Harper, D. B., Cook, A. L., Powell, K. A., Vaughan, M. A., and Winker, D. M.: Assessment of the CALIPSO Lidar 532 nm attenuated backscatter calibration using the NASA LaRC airborne High Spectral Resolution Lidar, Atmospheric Chemistry and Physics, 11, 1295–1311, https://doi.org/10.5194/acp-11-1295-2011, 2011.

Seifert, P., Kalesse-Los, H., Radenz, M., Gaudek, T., Ansmann, A., Macke, A., McDonald, A., and Coulson, G.: Investigation of aerosol effects on precipitation initiation processes in the alternately clean and aerosol-laden environment of New Zealand Aotearoa, in: PrePEP Conference: Precipitation Processes - Estimation and Prediction (PrePEP 2025), https://doi.org/10.5281/zenodo.15735777, 2025.

Smirnov, A., Holben, B. N., Slutsker, I., Giles, D. M., McClain, C. R., Eck, T. F., Sakerin, S. M., Macke, A., Croot, P., Zibordi, G., Quinn, P. K., Sciare, J., Kinne, S., Harvey, M., Smyth, T. J., Piketh, S., Zielinski, T., Proshutinsky, A., Goes, J. I., Nelson, N. B., Larouche, P., Radionov, V. F., Goloub, P., Krishna Moorthy, K., Matarrese, R., Robertson, E. J., and Jourdin, F.: Maritime Aerosol Network as a component of Aerosol Robotic Network, Journal of Geophysical Research: Atmospheres, 114, https://doi.org/https://doi.org/10.1029/2008JD011257, 2009.

Stein, A. F., Draxler, R. R., Rolph, G. D., Stunder, B. J. B., Cohen, M. D., and Ngan, F.: NOAA's HYSPLIT Atmospheric Transport and Dispersion Modeling System, Bulletin of the American Meteorological Society, 96, 2059–2077, https://doi.org/10.1175/BAMS-D-14-00110.1, 2015.

Stoffelen, A., Pailleux, J., Källén, E., Vaughan, J. M., Isaksen, L., Flamant, P., Wergen, W., Andersson, E., Schyberg, H., Culoma, A., Meynart, R., Endemann, M., and Ingmann, P.: THE ATMOSPHERIC DYNAMICS MISSION FOR GLOBAL WIND FIELD MEASUREMENT, Bulletin of the American Meteorological Society, 86, 73–88, https://doi.org/10.1175/BAMS-86-1-73, 2005.

Sun, K., Wu, S., Dai, G., Wang, X., Liu, B., Reitebuch, O., and Baars, H.: Aeolus L2B products validation with ground-based CDLs net over China and products application on aerosol observation, in: Aeolus Science Conference 2023, European Space Agency, https://www.aeolus2023.org/detailed-agenda, (last access: 20 February 2026), 2023.

Tesche, M., Groß, S., Ansmann, A., Müller, D., Althausen, D., Freudenthaler, V., and Esselborn, M.: Profiling of Saharan dust and biomass-burning smoke with multiwavelength polarization Raman lidar at Cape Verde, Tellus B, 63, 649–676, https://doi.org/10.1111/j.1600-0889.2011.00548.x, 2011.

Tesche, M., Wandinger, U., Ansmann, A., Althausen, D., Müller, D., and Omar, A. H.: Ground-based validation of CALIPSO observations of dust and smoke in the Cape Verde region, Journal of Geophysical Research: Atmospheres, 118, 2889–2902, https://doi.org/10.1002/jgrd.50248, 2013.

Thorsen, T. J., Fu, Q., and Comstock, J.: Comparison of the CALIPSO satellite and ground-based observations of cirrus clouds at the ARM TWP sites, Journal of Geophysical Research: Atmospheres, 116, https://doi.org/10.1029/2011JD015970, 2011.

Trapon, D., Baars, H., Floutsi, A. A., Bley, S., Haarig, M., Lacour, A., Flament, T., Dabas, A., Nehrir, A. R., Ehlers, F., and Huber, D.: Cross-validations of the Aeolus aerosol products and new developments with airborne high-spectral-resolution lidar measurements above the tropical Atlantic during JATAC, Atmospheric Measurement Techniques, 18, 3873–3896, https://doi.org/10.5194/amt-18-3873-2025, 2025.

van Zadelhoff, G.-J., Donovan, D. P., and Wang, P.: Detection of aerosol and cloud features for the EarthCARE atmospheric lidar (ATLID): the ATLID Feature Mask (A-FM) product, Atmospheric Measurement Techniques, 16, 3631–3651, https://doi.org/10.5194/amt-16-3631-2023, 2023.

Veselovskii, I., Goloub, P., Podvin, T., Bovchaliuk, V., Derimian, Y., Augustin, P., Fourmentin, M., Tanre, D., Korenskiy, M., Whiteman, D. N., Diallo, A., Ndiaye, T., Kolgotin, A., and Dubovik, O.: Retrieval of optical and physical properties of African dust from multi-wavelength Raman lidar measurements during the SHADOW campaign in Senegal, Atmospheric Chemistry and Physics, 16, 7013–7028, https://doi.org/10.5194/acp-16-7013-2016, 2016.

Voudouri, K. A., Siomos, N., Gkikas, A., Baars, H., Marinou, E., Paschou, P., and Amiridis, V.: Investigating the performance of Aeolus L2A products over Europe with Earlinet ground-based lidars, IEEE Xplore, IGARSS 2024 - 2024 IEEE International Geoscience and Remote Sensing Symposium, Athens, Greece, 07-12 July 2024, pp. 3100–3103, https://doi.org/10.1109/IGARSS53475.2024.10641977, 2024.

Wahl, S., Kanngießer, F., Leuzinger, A., Sudarchikova, N., Waza, A., and Fiedler, S.: PortMeteO sun photometer measurements during METEOR cruise M207, https://doi.org/10.1594/PANGAEA.983120, 2025.

Wandinger, U., Freudenthaler, V., Baars, H., Amodeo, A., Engelmann, R., Mattis, I., Groß, S., Pappalardo, G., Giunta, A., D'Amico, G., Chaikovsky, A., Osipenko, F., Slesar, A., Nicolae, D., Belegante, L., Talianu, C., Serikov, I., Linné, H., Jansen, F., Apituley, A., Wilson, K. M., de Graaf, M., Trickl, T., Giehl, H., Adam, M., Comerón, A., Muñoz-Porcar, C., Rocadenbosch, F., Sicard, M., Tomás, S., Lange, D., Kumar, D., Pujadas, M., Molero, F., Fernández, A. J., Alados-Arboledas, L., Bravo-Aranda, J. A., Navas-Guzmán, F., Guerrero-Rascado, J. L., Granados-Muñoz, M. J., Preißler, J., Wagner, F., Gausa, M., Grigorov, I., Stoyanov, D., Iarlori, M., Rizi, V., Spinelli, N., Boselli, A., Wang, X., Lo Feudo, T., Perrone, M. R., De Tomasi, F., and Burlizzi, P.: EARLINET instrument intercomparison campaigns: Overview on strategy and results, Atmospheric Measurement Techniques, 9, 1001–1023, https://doi.org/10.5194/amt-9-1001-2016, 2016.

Wandinger, U., Floutsi, A. A., Baars, H., Haarig, M., Ansmann, A., Hünerbein, A., Docter, N., Donovan, D., van Zadelhoff, G.-J., Mason, S., and Cole, J.: HETEAC – the Hybrid End-To-End Aerosol Classification model for EarthCARE, Atmospheric Measurement Techniques, 16, 2485–2510, https://doi.org/10.5194/amt-16-2485-2023, 2023a.

Wandinger, U., Haarig, M., Baars, H., Donovan, D., and van Zadelhoff, G.-J.: Cloud top heights and aerosol layer properties from EarthCARE lidar observations: the A-CTH and A-ALD products, Atmospheric Measurement Techniques, 16, 4031–4052, https://doi.org/10.5194/amt-16-4031-2023, 2023b.

Wandinger, U., Floutsi, A., Baars, H., Haarig, M., Hofer, J., Hünerbein, A., Bley, S., van Zadelhoff, G.-J., Donovan, D., Docter, N., and Preusker, R.: EarthCARE aerosol products and their validation needs, in: ACTRIS Science Conference 2024, 2024.

Wehr, T., Kubota, T., Tzeremes, G., Wallace, K., Nakatsuka, H., Ohno, Y., Koopman, R., Rusli, S., Kikuchi, M., Eisinger, M., Tanaka, T., Taga, M., Deghaye, P., Tomita, E., and Bernaerts, D.: The EarthCARE mission – science and system overview, Atmospheric Measurement Techniques, 16, 3581–3608, https://doi.org/10.5194/amt-16-3581-2023, 2023.

Weinzierl, B., Ansmann, A., Prospero, J. M., Althausen, D., Benker, N., Chouza, F., Dollner, M., Farrell, D., Fomba, W. K., Freudenthaler, V., Gasteiger, J., Groß, S., Haarig, M., Heinold, B., Kandler, K., Kristensen, T. B., Mayol-Bracero, O. L., Müller, T., Reitebuch, O.,

Sauer, D., Schäfler, A., Schepanski, K., Spanu, A., Tegen, I., Toledano, C., and Walser, A.: The Saharan Aerosol Long-Range Transport and Aerosol–Cloud-Interaction Experiment: Overview and Selected Highlights, Bulletin of the American Meteorological Society, 98, 1427–1451, https://doi.org/10.1175/BAMS-D-15-00142.1, 2017.

Winker, D. M., Pelon, J., Coakley, J. A., Ackerman, S. A., Charlson, R. J., Colarco, P. R., Flamant, P., Fu, Q., Hoff, R. M., Kittaka, C., Kubar, T. L., Treut, H. L., Mccormick, M. P., Mégie, G., Poole, L., Powell, K., Trepte, C., Vaughan, M. A., and Wielicki, B. A.: The CALIPSO Mission: A Global 3D View of Aerosols and Clouds, Bulletin of the American Meteorological Society, 91, 1211–1230, https://doi.org/10.1175/2010BAMS3009.1, 2010.

Witschas, B., Lemmerz, C., Geiß, A., Lux, O., Marksteiner, U., Rahm, S., Reitebuch, O., and Weiler, F.: First validation of Aeolus wind observations by airborne Doppler wind lidar measurements, Atmospheric Measurement Techniques, 13, 2381–2396, https://doi.org/10.5194/amt-13-2381-2020, 2020.

Wu, D., Wang, Z., Wang, B., Zhou, J., and Wang, Y.: CALIPSO validation using ground-based lidar in Hefei (31.9° N, 117.2° E), China, Applied Physics B, 102, 185–195, https://doi.org/10.1007/s00340-010-4243-z, 2011.

Yin, Z. and Baars, H.: PollyNET/Pollynet Processing Chain: Version 3.0, https://doi.org/10.5281/zenodo.5571289, 2021.

Yorks, J. E., McGill, M. J., Palm, S. P., Hlavka, D. L., Selmer, P. A., Nowottnick, E. P., Vaughan, M. A., Rodier, S. D., and Hart, W. D.: An overview of the CATS level 1 processing algorithms and data products, Geophysical Research Letters, 43, 4632–4639, https://doi.org/10.1002/2016GL068006, 2016.